A Chemical Genetic Approach Reveals Distinct Mechanisms of EphB Signaling During Brain Development

Published in final edited form as:
Nat Neurosci. 2012 December ; 15(12): 1645–1654. doi:10.1038/nn.3249.

A Chemical Genetic Approach Reveals Distinct Mechanisms of EphB Signaling During Brain Development

Michael J. Soskis[1,*], **Hsin-Yi Henry Ho**[1,*], **Brenda L. Bloodgood**[1], **Michael A. Robichaux**[4], **Athar N. Malik**[1], **Bulent Ataman**[1], **Alex A. Rubin**[1], **Janine Zieg**[1], **Chao Zhang**[2,3], **Kevan M. Shokat**[2], **Nikhil Sharma**[1], **Christopher W. Cowan**[4,5], and **Michael E. Greenberg**[1,‡]

[1]Department of Neurobiology, Harvard Medical School, Boston, MA

[2]Department of Cellular and Molecular Pharmacology, University of California, San Francisco, CA

[4]Department of Psychiatry, University of Texas Southwestern Medical Center, Dallas, TX

Abstract

EphB receptor tyrosine kinases control multiple steps in nervous system development. However, it remains unclear whether EphBs regulate these different developmental processes directly or indirectly. In addition, as EphBs signal through multiple mechanisms, it has been challenging to define which signaling functions of EphBs regulate particular developmental events. To address these issues, we engineered triple knockin mice in which the kinase activity of three neuronally expressed EphBs can be rapidly, reversibly, and specifically blocked. Using these mice we demonstrate that the tyrosine kinase activity of EphBs is required for axon guidance in vivo. By contrast, EphB-mediated synaptogenesis occurs normally when the kinase activity of EphBs is inhibited suggesting that EphBs mediate synapse development by an EphB tyrosine kinase-independent mechanism. Taken together, these experiments reveal that EphBs control axon guidance and synaptogenesis by distinct mechanisms, and provide a new mouse model for dissecting EphB function in development and disease.

INTRODUCTION

The EphB family of receptor tyrosine kinases (RTKs) are critical regulators of cell-cell contacts in the developing nervous system, mediating processes as diverse as axon guidance, topographic mapping, neuronal migration, and synapse formation[1–3]. In addition to these developmental roles, EphB dysfunction in the mature organism contributes to pathologies such as cancer, Alzheimer's disease, and possibly autism [4–8]. The signaling mechanisms underlying EphB-mediated development and disease are largely unknown.

Since the EphB family of receptors has been shown to regulate a large number of developmental processes, it has been particularly difficult to determine the specific functions of EphBs at defined times during brain development. The presence of at least three partially

[‡]To whom correspondence should be addressed: Harvard Medical School, Department of Neurobiology, Goldenson Building, Room 420, 220 Longwood Avenue, Boston, MA 02115, Phone: 617-432-1772, FAX: 617-734-7557, michael_greenberg@hms.harvard.edu.
[3]Present Address: Department of Chemistry, University of Southern California, Los Angeles, CA
[5]Current address: Department of Psychiatry, McLean Hospital, Harvard Medical School, Belmont, MA
[*]These authors contributed equally to this work.

AUTHOR CONTRIBUTIONS

M.J.S., H.-Y.H.H., and M.E.G. conceived and designed the study. M.J.S. and H.-Y.H.H conducted all of the experiments unless otherwise noted. B.L.B. and N.S. performed electrophysiological recordings. J.Z. generated EphB1 and EphB3 targeting constructs. M.A.R. and C.W.C. contributed to axon guidance experiments. A.N.M. and A.A.R. generated shRNAs for EphBs. B.A. performed qPCR experiments. C.Z. and K.M.S. designed and synthesized inhibitors. M.J.S., H.-Y.H.H., and M.E.G. wrote the manuscript.

redundant EphB family members in the nervous system further complicates investigation into the biological functions of EphB proteins. For example, the *Ephb1, Ephb2*, and *Ephb3* single and compound mutant mice display defects in a number of processes including stem cell proliferation, axon guidance, filopodial motility, dendritic spine formation, synapse development, and long-term potentiation (LTP), but it is unclear which of these interdependent phenotypes are direct and which are secondary to the disruption of EphB signaling at an earlier developmental step[9–13].

Another major hurdle in understanding the function of EphBs is the complex nature of their signaling capabilities. EphBs can engage in bidirectional signaling with their transmembrane ligands, the ephrin-Bs. In the forward direction of signaling, the interaction of clustered ephrin-B ligands on one cell with EphB receptors on another leads to EphB oligomerization and auto-phosphorylation, the induction of EphB kinase activity, and the recruitment of cytoplasmic proteins via SH2-binding and PDZ-binding motifs of EphBs[14]. In addition, the extracellular region of EphBs, which contains fibronectin repeat domains, can recruit binding partners such as subunits of the NMDA subtype of glutamate receptor[15,16]. In the reverse direction of EphB/ephrin-B signaling, phosphorylation of the cytoplasmic tail of ephrin-Bs results in the recruitment of SH2-domain containing proteins and initiation of downstream signal transduction [17]. Thus, through a complex array of potential signaling pathways, EphBs are able to mediate a wide range of processes during nervous system development.

For the most part, it remains to be determined which cellular processes require EphB receptor tyrosine kinase activity, and which cellular responses are mediated by EphB tyrosine kinase-independent signaling events. Cytoplasmic deletions of EphBs have been used to assess the requirement of the intracellular domain in mediating specific EphB-regulated processes, but this approach fails to distinguish kinase activity from other modes of cytoplasmic signaling[18]. In particular, since ephrin-B binding to EphBs induces the formation of EphB oligomers within the plasma membrane, it remains a likely possibility that EphB oligomerization and scaffolding, in the absence of induction of EphB tyrosine kinase activity, mediates some of the biological effects of EphBs[14]. Thus, new ways of selectively inhibiting specific functions of EphBs are critically needed to clarify the kinase-dependent and kinase-independent mechanisms by which EphBs control specific developmental events such as axon guidance and synapse formation.

Much of what is currently known about the role of EphB signaling during axon guidance in vivo comes from studies of retinal and cortical axon tracts. Notably, genetic deletions of individual or combinations of EphB family members cause profound axon guidance defects that result in the abnormal formation of several axon tracks, including the ipsilateral retinocollicular projection as well as axonal tracts in the corpus callosum and the anterior commissure[9,19]. However, it remained to be determined whether EphB-dependent axon guidance decisions are mediated by the kinase activity of EphBs or rather by other modes of EphB signaling, such as PDZ-domain interactions, cytoplasmic domain oligomerization, reverse signaling through ephrin-Bs, or EphB extracellular domain interactions.

In general, the mechanisms by which the cytoplasmic domains of axon guidance receptors signal growth cone attraction or repulsion have been difficult to identify. Most axon guidance receptors that have been studied to date, such as Robo, DCC, plexins and neuropilins, do not possess intrinsic kinase activity, suggesting that the predominant mode of axon guidance signaling may be kinase independent[20]. With regard to EphBs, studies in the visual system have implicated a role for the kinase activity, while studies in the cortex have suggested kinase-independent roles of EphBs[9,21–24]. However, none of these

experiments were able to directly address the requirement of the kinase activity of EphBs when they are expressed at endogenous levels in vivo.

In additional to their function in axon guidance, EphBs have been shown to play a key role in cortical and hippocampal synapse formation. *Ephb* knockout mice or knockin mice with cytoplasmic domain deletions display defects in dendritic spine and synapse development in dissociated neuronal cultures and in hippocampal slices[13,18]. Overexpression of kinase-defective dominant negative mutants also results in abnormal spine and synapse development, suggesting a role for the tyrosine kinase activity of EphBs in these processes[13,15,25]. However, these previous studies have not directly tested the requirement of the kinase activity of EphBs in the regulation of synapse formation under conditions where ephrin-Bs and EphBs are expressed at physiological levels, thus complicating the interpretation of the findings and leaving open the possibility that aspects of EphB-dependent synapse development may be kinase-independent.

To address the importance of the kinase activity of EphBs for axon guidance and synapse development, we combined chemical biology with mouse genetic engineering to reversibly inhibit EphB tyrosine kinase signaling in cultured neurons, brain slices, and live animals. By mutating a bulky gatekeeper residue in the ATP-binding pocket of EphBs to a smaller alanine or glycine, we rendered the enzymatic activity of these kinases sensitive to reversible inhibition by derivatives of the Src inhibitor PP1. These analogs of PP1 do not fit into the ATP-binding pocket of wild-type kinases[26,27] and thus do not inhibit wild-type EphBs or other kinases. In a previous study, this approach was successfully employed to regulate Trk receptor tyrosine kinase signaling[28]. We reasoned that this approach would be particularly well suited to investigate the more complex EphB family, allowing us to inhibit the kinase activity of EphBs while preserving extracellular interactions, reverse signaling, or other cytoplasmic domain functions of EphBs.

We generated a triple knockin mouse line that harbors ATP binding pocket mutations in EphB1, EphB2 and EphB3. By specifically blocking the kinase function of EphBs in these knockin mice in a temporally controlled manner, we demonstrate for the first time a requirement for the kinase activity of EphBs in axonal guidance in vivo. By contrast, the kinase activity of EphBs is not required for another key EphB-mediated event, the regulation of excitatory synapse formation. Thus, when expressed under physiologically relevant conditions, EphBs differentially regulate key aspects of neuronal development by kinase-dependent and -independent mechanisms.

RESULTS

A Chemical Genetic Approach to Studying EphB Signaling

To selectively inhibit the tyrosine kinase activity of EphBs, we employed a strategy that combines the advantages of both pharmacology and genetics in which drug-sensitivity can be engineered into a protein[29,30]. The ATP-binding pocket of all kinases contains a bulky hydrophobic gatekeeper residue that is not essential for the catalytic function of the kinase domain. However, this gatekeeper residue, when mutated to an alanine or a glycine, can render the kinase sensitive to inhibition by PP1 analogs that cannot effectively enter the wild type ATP-binding pocket (Fig. 1a)[29,30]. As described below, we have engineered EphBs with modified gatekeeper residues and will refer to these PP1 analog sensitive (AS) EphBs as AS-EphBs.

To design AS-EphB mutants, we compared the amino acid sequence of kinase domains of EphBs with those of related tyrosine kinases for which AS versions had been successfully made[26,28]. This analysis revealed a gatekeeper threonine residue in the ATP-binding pocket

of mouse EphB1, EphB2 and EphB3 (Fig. 1b). We substituted these residues with either alanine or glycine to generate *Ephb1*^{T697G}, *Ephb2*^{T699A}, and *Ephb3*^{T706A}.

To verify that the mutations introduced into the EphB ATP-binding pockets did not affect the kinase activity of EphBs in the absence of the PP1 analogs, we assessed the activity of these kinases using a heterologous cell culture system. Activation of EphBs results in receptor auto-phosphorylation on several juxtamembrane tyrosine residues. We previously generated an antibody that specifically recognizes the phosphorylated form of these juxtamembrane tyrosine residues for all EphBs, and used the juxtamembrane tyrosine phosphorylation detected by this anti-phospho EphB antibody as a readout for receptor kinase activation[15]. We overexpressed EphBs in HEK 293 cells where EphBs cluster spontaneously and become activated in a ligand-independent manner. We probed lysates from cells overexpressing AS-EphBs or wild-type EphBs with the anti-phospho-EphB antibody, and found that wild-type and AS-EphBs are phosphorylated at their juxtamembrane tyrosines to a similar extent (Fig. 1c). This result indicates that the AS mutation does not affect the ability of EphBs to activate their kinase domains in the absence of PP1 analogs.

To test the ability of PP1 analogs to inhibit AS-EphBs, we treated HEK 293 cells overexpressing AS-EphBs or wild type EphBs with either of two bulky PP1 analogs, 4-amino-1-*tert*-butyl-3-(1′naphthyl)pyrazolo[3,4-*d*]pyrimidine (1-NA-PP1) or 1-(*tert*-Butyl)-3-(3-methylbenzyl)-1H-pyrazolo[3,4-d]pyrimidin-4-amine (3-MB-PP1) (Fig. 1a) and assessed EphB tyrosine phosphorylation. We found that incubation with 1-NA-PP1 (250nM) or 3-MB-PP1 (1μM) blocked the phosphorylation of AS-EphBs but not the phosphorylation of wild-type EphBs (Fig. 1c). The drug vehicle DMSO alone did not have any effect on either wild-type or AS-EphBs. These results indicate that the kinase activity of AS-EphBs is selectively inhibited by PP1 analogs. Inhibition of kinase activity of AS-EphBs was rapid, occurring within minutes (Fig. 1d). Since PP1 analogs act competitively, inhibition was readily reversible upon removal of 1-NA-PP1 (Fig. 1e). The specificity, rapidity and reversibility of the kinase inhibition render the chemical genetic strategy an ideal platform for studying dynamic biological processes in cells and animals.

To quantify the potency and specificity of 1-NA-PP1 and 3-MB-PP1 with respect to inhibition of EphB1, EphB2 and EphB3, we conducted dose-response analyses. We determined the IC50s of kinase inhibition, which revealed a preference of the PP1 analogs for inhibiting AS kinases (9–48 nM) over wild-type kinases (0.6–8.9 μM) by two orders of magnitude (Supplementary Fig. 1a, b). These results indicate that the kinase activity of AS-EphBs is selectively inhibited by PP1 analogs.

To confirm that binding of PP1 analogs to AS-EphBs does not affect kinase-independent aspects of EphB function, we performed in vitro binding assays to compare the effect of 1-NA-PP1 on tyrosine kinase-dependent and -independent protein-protein interactions. The SH2 and SH3 domain-containing adaptor protein Grb2 is a classic example of a signaling molecule that interacts with RTKs, including EphBs, through a tyrosine kinase-dependent mechanism. Upon receptor activation and auto-phosphorylation, the phospho-tyrosine residues in the cytoplasmic tails of RTKs, including EphBs, recruit Grb2 through its SH2 domain[3132]. By contrast, binding of the PDZ domain-containing protein Pick1 to EphBs occurs through the C-terminal PDZ domain-binding motif of EphBs and does not require the tyrosine kinase activity of EphBs[33]. In the binding experiments, we found that EphB1 binds strongly to both GST-Grb2 and GST-Pick1, but not the negative control GST alone (Fig. 1f). Importantly, while 1-NA-PP1 (1μM) completely abolished the kinase-dependent interaction between AS-EphB1 and GST-Grb2, the inhibitor treatment had no effect on the kinase-independent interaction between AS-EphB1 and GST-Pick1 (Fig. 1f). These observations

thus provide evidence that 1-NA-PP1 specifically targets kinase-dependent functions of EphB proteins.

Generation and Validation of AS-EphB TKI mice

Encouraged by these initial experiments, we generated knockin mice harboring the gatekeeper mutation in EphB1 (T697G), EphB2 (T699A), and EphB3 (T706A), the three catalytically-active EphB receptor tyrosine kinases expressed in the developing brain. *Ephb1*^{T697G}, *Ephb2*^{T699A}, and *Ephb3*^{T706A} single mutant mice were generated individually by homologous recombination in mouse embryonic stem (ES) cells (Supplementary Fig. 1a, b, c). ES cell clones were confirmed by sequencing the targeted alleles in ES cells (Fig. 2a).

Previous studies have demonstrated significant functional redundancy of EphBs in several contexts[18,22,34]. To overcome potential compensation by different EphB family members, *Ephb1*^{T697G}, *Ephb2*^{T699A}, and *Ephb3*^{T706A} single mutants were intercrossed to generate a line that is triply homozygous for each of the targeted EphB alleles, here designated EphB triple knockin (AS-EphB TKI) mice.

Whereas *Ephb1/Ephb2/Ephb3* triple knockout mice suffer from profound developmental defects, including morphological abnormalities of the palate and the anogenital region[35,36], AS-EphB TKI mice develop normally into healthy, fertile adults, indistinguishable from wild-type mice. Notably, AS-EphB TKI brains exhibit normal morphology and are of equal size to wild-type mouse brains. In vitro assays measuring axon guidance, neuronal morphology, and synaptic development revealed no differences between wild-type and AS-EphB TKI mice (shown below), suggesting that AS-EphBs function normally in the absence of PP1 analogs.

Critical to the interpretation of experiments comparing wild-type and AS-EphB TKI mice is evidence that EphB mRNA expression, trafficking, and ligand-mediated receptor activation occur normally in AS-EphB TKI neurons in the absence of PP1 analogues. First, we performed quantitative PCR (qPCR) to measure expression of the *Ephb1, Ephb2* and *Ephb3* mRNAs in neurons from wild-type and AS-EphB TKI mice. We found that mRNAs isolated from the mutant alleles were expressed at the same levels as wild-type (Fig. 2b). We conclude that the gene targeting did not affect the level of *Ephb1, Ephb2* and *Ephb3* mRNA expression in AS-EphB TKI neurons.

We next asked whether neurons from AS-EphB TKI mice could engage in ephrin-B-induced signaling. We cultured dissociated cortical neurons from embryonic day 16.5 to 18.5 (E16.5–18.5) AS-EphB TKI or wild-type mice and stimulated the neurons with clustered ephrin-B1 for 30 minutes. Western blotting of AS-EphB TKI or wild-type lysates with the anti-phospho-EphB antibody revealed that both wild-type and AS-EphB TKI neurons exhibited robust EphB activation to similar levels, indicating that AS-EphBs are fully competent to engage in ephrin-B-induced kinase signaling in the absence of PP1 analogs (Fig. 3a).

To test whether the kinase function of endogenously expressed EphBs from AS-EphB TKI mice can be effectively and selectively inhibited by PP1 analogs, we pre-incubated cultured E16.5-E18.5 neurons with vehicle or PP1 analogs for 1 hour before ephrin-B1 stimulation. Treatment with 250 nM 1-NA-PP1 or 1 μM 3-MB-PP1 completely abolished ephrin-B1-induced EphB activation in the AS-EphB TKI, but not wild-type cells, thus demonstrating the efficacy and selectivity of these PP1 analogs for AS-EphBs expressed at endogenous levels in neurons (Fig. 3a).

To more rigorously test the selectivity of PP1 analogs, we assessed the effect of these inhibitors on the kinase activity of EphA4, one of the closest relatives of EphBs. We stimulated wild-type cortical neurons that had been pre-incubated with 250 nM 1-NA-PP1 or 1 μM 3-MB-PP1 with the EphA4 ligand ephrin-A1, immunoprecipitated EphA4 with an anti-EphA4 antibody and analyzed the immunoprecipiates for phospho-EphA4 or total EphA4. We found no inhibition of EphA4 autophosphorylation at concentrations of PP1 analogs that fully block AS-EphB tyrosine kinase function (Fig. 3b). The specificity of AS inhibition between subfamilies of Eph receptors contrasts with previous unsuccessful attempts at designing selective inhibitors for EphBs relative to EphAs[37,38].

To determine whether PP1 analogs affect the cell surface expression or internalization of AS-Eph proteins, we performed surface biotin labeling for the EphB2 receptor after chronic inhibition from 6–12 days in vitro (DIV) in cortical neurons. We found equivalent levels of labeled EphB2 in vehicle and 1-NA-PP1 (1 μM)-treated cells (Supplementary Fig. 3). This result indicates that surface expression of EphBs is not altered by the inhibitor treatment.

Kinase cascades can amplify signals greatly. To test whether inhibition of the kinase activity of EphBs effectively blocked the phosphorylation of downstream tyrosine kinase substrates, we examined phosphorylation of the well-characterized EphA and EphB substrate Vav2, a Rho family guanine nucleotide exchange factor (GEF) that mediates growth cone collapse[39]. Wild-type or AS-EphB TKI neurons were incubated in 1-NA-PP1 (250 nM) or 3-MB-PP1 (1 μM) and stimulated with ephrin-B1 for 30 minutes to induce Vav2 tyrosine phosphorylation. Immunoprecipitation of Vav2 followed by Western blotting with a pan-phospho-tyrosine antibody showed a significant increase in tyrosine phosphorylation of Vav2 after ephrin-B1 stimulation (Fig. 3c, d). Treatment with 1-NA-PP1 (250 nM) or 3-MB-PP1 (1 μM) selectively blocked the increase in Vav2 phosphorylation in AS-EphB TKI cells, but had no effect in wild-type cells (Fig. 3c, d). We conclude that PP1 analogs can selectively block the kinase signaling of EphBs and the phosphorylation of their substrates in AS-EphB TKI cells.

EphB RTK signaling is required for growth cone collapse

EphBs have classically been studied in the context of axon guidance[40,22,41]. While some studies have implicated a role for the kinase activity of EphBs in axon guidance, others have suggested kinase-independent modes of EphB signaling[9,21–24]. To assess the role of EphB kinase activity in axon guidance, we initially chose the visual system because the importance of EphBs in this system is well established. During development of the visual system, most retinal ganglion cell (RGC) axons emanating from the retina enter and cross the optic chiasm at the midline to form the contralateral retinal projections in the lateral geniculate nucleus (LGN) and superior colliculus (SC)[40,24]. However, RGC axons from the ventrotemporal (VT) region of the retina, which express EphB1, become repelled by the ephrin-B2-expressing glia of the optic chiasm and form the ipsilateral projection that is required for stereovision[42]. Ephrin-B2 is thought to repel EphB1 expressing axons by inducing the collapse of their growth cones, an activity that can be recapitulated in vitro.

To begin to address whether the kinase activity of EphBs is required for repulsive axon guidance, we asked whether the kinase activity of EphBs is required for growth cone collapse. We prepared explants from E14 VT retinae and visualized growth cones with fluorescently conjugated phalloidin (to label F-actin) and axons with anti-neurofilament staining. In these explants, RGCs extend axons with broad, fan-shaped growth cones over a laminin substrate. We measured the state of growth cones by two methods: first, growth cones were scored as collapsed if they exhibited rod-like morphology and lacked visible lamellipodia. This method allowed us to quantify the percentage of growth cones that were

collapsed in each explant. Second, we measured the maximum axial width of each growth cone and calculated the average axial width of the growth cones in each explant.

When treated with clustered ephrin-B2, growth cones from AS-EphB TKI explants exhibit a robust collapse response (Fig. 4a, b). Treatment of AS-EphB TKI explants with 1-NA-PP1 (250 nM) or 3-MB-PP1 (1 μM) led to a dramatic decrease in the percentage of collapsed growth cones upon ephrin-B treatment (Fig. 4a, b). In addition, AS-EphB TKI explants showed an ephrin-B2-induced decrease in growth cone width in vehicle-treated explants, but only a slight reduction in explants exposed to 1-NA-PP1 or 3-MB-PP1 (Fig. 4c). This drug-dependent blockade of growth cone collapse was not seen in wild-type explants: wild-type cells showed a robust collapse regardless of the presence of inhibitors as well as a significant reduction in average growth cone width after stimulation (Fig. 4a–c). Based on these results, we conclude that the kinase activity of EphBs is required for ephrinB-induced RGC growth cone collapse.

To verify that treatment of explants with 1-NA-PP1 and 3-MB-PP1 led to inhibition of ephrin-B-dependent EphB tyrosine phosphorylation in RGC axons, we stained explants with the anti-phospho-EphB antibody. In the absence of stimulation, minimal phospho-EphB staining was observed in growth cones from wild-type or AS-EphB TKI explants (Fig. 4a). Upon ephrin-B2 stimulation, punctate patterns of anti-phospho-EphB antibody staining were seen in the growth cone and along the axon (Fig. 4a). This staining was blocked in 1-NA-PP1 (250 nM) or 3-MB-PP1 (1 μM)-treated AS-EphB TKI explants, but not in wild-type explants, indicating that PP1 analogs selectively inhibit the kinase activity of EphBs in AS-EphB TKI RGC explants (Fig. 4a).

A crucial feature of the chemical genetic approach is the reversibility of kinase inhibition. To test whether the inhibitory effect of 1-NA-PP1 on growth cone collapse is indeed reversible, we removed 1-NA-PP1 midway through a 30-minute ephrin-B2 stimulation in AS-EphB TKI explants. Whereas in the presence of 1-NA-PP1, ephrin-B-stimulated growth cones did not collapse, after washout growth cones rapidly collapsed (Fig. 4d). This finding demonstrates the reversibility of PP1 analog inhibition of growth cone collapse in retinal explants from AS-EphB TKI mice and rules out a general health issue as a cause of reduced growth cone collapse.

EphB RTK signaling mediates retinal axon guidance in vivo

Having established the requirement of the tyrosine kinase activity of EphBs for growth cone collapse in vitro, we next asked whether this requirement is relevant for repulsive guidance in vivo, where growth cones exhibit salutatory motion rather than simple extension and collapse. In addition, growth cone collapse in vivo is mediated by a number of cues, among them membrane bound ephrin-B rather than ectopically added aggregated soluble ephrin-Bs

To determine whether the kinase activity of EphBs is required for the repulsive guidance of axons under physiological conditions of ephrin-B/EphB signaling in vivo, we examined the effect of inhibiting the kinase activity of EphBs on axon repulsion at the optic chiasm. We treated pregnant mice with 1-NA-PP1 from E13.5–16.5, the time when RGC axons encounter the optic chiasm (Fig 5a) and analyzed the retinal projections at E16.5 by DiI labeling.

To assess the degree of ipsilateral vs. contralateral retinal projection, we measured the fluorescence intensity of a rectangular region in the ipsilateral projection and divided this by the total fluorescence intensity in the combined ipsilateral and contralateral projections to derive the Ipsilateral Index (Fig. 5b)[40]. In 1-NA-PP1-treated AS-EphB TKI embryos, we found that the ipsilateral retinal projection was strongly reduced (by 42%) compared to

untreated AS-EphB TKI embryos (Fig. 5c, d). In many of the AS-EphB TKI embryos treated with 1-NA-PP1, the ipsilateral projection was absent. By contrast, 1-NA-PP1 treatment had no effect on the ipsilateral retinal projection in wild-type embryos, indicating that the observed guidance deficit was due to specific inhibition of EphBs (Fig. 5c, d). These experiments provide evidence that the tyrosine kinase activity of EphBs is required for axon repulsion at the optic chiasm. They also illustrate the utility of AS-EphB mice for examining the importance of the tyrosine kinase activity of EphBs in both in vitro and in vivo settings. Our results demonstrate that PP1 analogs are capable of entering the brain tissue of an intact organism and then effectively and potently inhibiting EphB tyrosine kinase activity. These analogues also completely inhibit EphB tyrosine kinase activity in neuronal cultures making it possible to use the AS-EphB TKI neurons to investigate the role of the kinase activity of EphBs in a diverse array of neuronal functions.

EphB RTK signaling mediates corpus callosum formation

Based on the finding that EphB tyrosine kinase activity mediates axon guidance at the optic chiasm, we next asked whether a similar mechanism might be used during other axon guidance decisions. We focused on the role of the tyrosine kinase activity of EphBs in the formation of the corpus callosum. Different EphB family members have been suggested to mediate this process through both forward and reverse signaling, but the requirement of the kinase activity has not been tested[22,43]. To address this question, we administered 1-NA-PP1 to pregnant AS-EphB TKI mice from E12.5–19.0 and visualized major axon tracts by L1-CAM staining (Fig. 6a). As expected, untreated AS-EphB TKI mice had normal corpus callossa (0/6 mice with agenesis) (Fig. 6b). However, AS-EphB TKI mice treated with 1-NA-PP1 all had partial corpus callosum agenesis with a gap in the dorsal midline region (11/11 mice (Fig. 6b). Wild-type mice treated with 1-NA-PP1 had a normal corpus callosum (0/6 mice), demonstrating that the corpus callosal agenesis phenotype was specific to inhibition of AS-EphBs (Fig. 6b). These data indicate that the tyrosine kinase activity of EphBs is essential for proper formation of the corpus callosum in vivo. Taken together with our findings on retinal axon guidance, these observations suggest that tyrosine kinase-dependent signaling is likely a general mechanism by which EphB forward signaling mediates repulsive axon guidance in vivo.

EphB RTK signaling is not required for synaptogenesis

In addition to their role in axon guidance, EphBs have been shown in numerous studies to control synapse development and function[12,13,15,16,18,25,44,45]. Experiments involving overexpression of kinase-defective EphB mutants and the use of knockin mice containing cytoplasmic truncations of EphBs have suggested a role for kinase signaling in synaptogenesis[12,13,15,18,25]. However, the relevance of the tyrosine kinase activity of EphBs for synaptogenesis has not been examined under conditions where ephrin-Bs and EphBs are expressed at endogenous levels and engage in physiological signaling.

The most profound synaptic defect observed after perturbation of EphB expression is the loss of dendritic spines, the sites on dendrites where most excitatory synapses form. In neurons from EphB1, EphB2 and EphB3 triple knockout mice, dendritic spine development is severely compromised[13,18]. To assess the importance of the tyrosine kinase activity of EphBs for spine development, cortical neurons were cultured from E15-E17 AS-EphB TKI or wild type embryos and treated with 1-NA-PP1 (1μM) between 10–21 DIV, the peak of spinogenesis. To ensure exposure to the full dose of the inhibitor during this long period, the culture medium was changed completely every three to four days with fresh 1-NA-PP1. To visualize the fine dendritic structures, neurons were transfected with GFP at 10 DIV and analyzed at 21 DIV. To assess spine density, we counted spines per unit dendritic length over multiple segments of dendrite totaling more than 50 μm in length. Notably, we found

that 1-NA-PP1 treatment had no significant effect on spine number and length in AS-EphB TKI or wild-type neurons (Fig. 7a, b). This result suggests that the tyrosine kinase activity of EphBs is not required for dendritic spine development in dissociated cortical neurons.

To functionally test the effect of 1-NA-PP1 on synaptogenesis, we measured miniature excitatory postsynaptic currents (mEPSCs) in dissociated cortical neurons from AS-EphB TKI mice in the presence or absence of 1-NA-PP1. These cultures were treated with 1 μM 1-NA-PP1 beginning at 3 DIV until 10–12 DIV, and mEPSCs were measured by whole cell electrophysiological recordings. Consistent with the spine analysis, we found no difference in mEPSC frequency or amplitude between AS-EphB TKI neurons treated with vehicle or 1-NA-PP1 (Fig. 7c, d), again strongly suggesting that the tyrosine kinase activity of EphBs is not required for synaptogenesis, at least in dissociated neurons.

To confirm that chronic 1-NA-PP1 treatment inhibits EphB tyrosine phosphorylation in these cultures, we performed Western analysis on concurrent cultures and found that exposure of AS-EphB TKI neurons to 1-NA-PP1 (1 μM) resulted in a complete inhibition of ephrin-B-induced EphB auto-phosphorylation (Fig. 7e).

To determine if the tyrosine kinase activity of EphBs might control excitatory synapse development or function in the context of a more intact neural circuit, we also examined the effect of 1-NA-PP1 inhibition on dendritic spine development, mEPSCs, and evoked excitatory postsynaptic currents (eEPSCs) in organotypic hippocampal slices prepared from AS-EphB TKI mice. Expression of shRNAs targeting *Ephb1, Ephb2* and *Ephb3* led to significant alterations in spine development (Supplementary Fig. 4a–c, 5a–d), mEPSC and eEPSC currents (Supplementary Fig. 6a–d) in organotypic hippocampal slice cultures indicating that EphBs play a significant role in excitatory synaptic development under these conditions. However, in sharp contrast to the findings with EphB shRNA, the addition of 1-NA-PP1 to slices from AS-EphB TKI mice had no effect on dendritic spine growth (Fig. 8a–d), mEPSC characteristics (Fig. 8e, f), or eEPSC events (Fig. 8g, h). Taken together these experiments suggest that at least under the conditions tested the tyrosine kinase activity of EphBs is not required for the formation or maintenance of functional synapses.

DISCUSSION

Employing a chemical genetic strategy, we have engineered mice in which it is possible to acutely, reversibly, and specifically inhibit the kinase signaling of EphBs in vitro and in vivo. We find that synaptogenesis, a process that requires EphB proteins, does not depend on the tyrosine kinase activity of EphBs. By contrast, we demonstrate a clear requirement for the tyrosine kinase activity of EphBs in ephrin-B-mediated growth cone collapse in culture and in the repulsive guidance of retinal and corpus callosal axons in vivo. Thus, unlike many other axon guidance receptors, EphBs mediate axon repulsion via a receptor tyrosine kinase-dependent mechanism.

Our finding that the kinase activity of EphBs is not required for the formation of excitatory synapses was unexpected and suggests a possible role for cytoplasmic domain oligomerization and other forms of protein-protein interactions in this process. For example, the binding of PDZ-domain containing synaptic proteins with the cytoplamic tail of EphBs or the recruitment of NMDA receptors via the EphB extracellular region may initiate or stabilize the formation of excitatory synapses[13,15]. Alternatively, EphBs could initiate signaling by recruiting other cytoplasmic kinases, such as the Src family of tyrosine kinases[44]. While our data strongly suggest that the tyrosine kinase activity of EphBs is not required for synaptogenesis under a wide range of experimental conditions tested, we cannot rule out the possibility that EphB kinase signaling plays a role in other contexts. It will be

important in future investigations to test whether the kinase activity of EphBs functions instead in the plasticity of these synapses, as multiple reports have identified a role for EphBs in long-term potentiation (LTP) in the hippocampus[10,11].

In contrast to synaptogenesis, our results reveal a requirement for the tyrosine kinase activity of EphBs in the formation of the ipsilateral retinal projection and the corpus callosum. Our finding that EphB tyrosine kinase activity is required for retinal guidance is consistent with a previous study showing that overexpression of EphB1 is sufficient to drive retinal axons to ectopically project ipsilaterally, and that this function requires an intact EphB1 kinase domain[23]. These findings are also consistent with a recent study in which a knockin mouse was made with the intracellular region of EphB1 replaced with lacZ[24]. This mouse displays a loss of the ipsilateral retinal projection and thus indicates that EphB forward signaling is necessary for the formation of the ipsilateral retinal projection. Through the use of AS-EphB TKI mice, we have now been able to directly implicate the tyrosine kinase activity of EphBs in the formation of the ipsilateral retinal projection.

Mutations of the cytoplasmic domains of EphBs or ephrin-Bs suggest that the formation of the corpus callosum is more complex than the ipsilateral retinal projection and could involve both EphB forward and reverse signaling[22]. However, our finding that inhibition of the kinase activity of EphBs in vivo results in a highly penetrant corpus callosum agenesis phenotype provides clear evidence for the requirement of EphB kinase signaling in the development of the corpus callosum.

Based on our observations, we favor a model in which the tyrosine kinase activity of EphBs is required for repulsive interactions such as in axon guidance, but may not be required for adhesive interactions such as axon fasciculation and synapse formation. This model is consistent with previous theories in which the amount of kinase activation predicts the strength of repulsion[46]. Furthermore, inhibiting kinase activity in a normally repulsive context (such as axon guidance) may lead to unnatural adhesion. Thus, it will be interesting to study the fate of the misprojected axons we observed in the optic tract and corpus callosum. It will also be important to search for any counterexamples to our model, such as an adhesive interaction that is EphB tyrosine kinase-dependent. The delicate balance between the opposing functionalities of the ephrin-B/EphB signaling system underscores the importance of studying these interactions under physiological conditions.

Understanding the downstream mechanism by which the tyrosine kinase activity of EphBs controls axon guidance represents an important direction for future studies. One crucial mediator of this signaling might be the Vav family of GEFs for the small GTPase Rac. Vav2 is known to control growth cone collapse, and *Vav2/3* double mutant mice display defects in the development of the ipsilateral retinocollicular projection[39,47]. In this study, we further demonstrate that the tyrosine kinase activity of EphBs is required for ephrin-B-induced Vav2 tyrosine phosphorylation. A thorough investigation of how EphBs control repulsive axon guidance will require knowledge of the full complement of tyrosine kinase substrates of EphBs. Since AS kinases accept orthologous ATP analogs that can directly label the targets of the kinase[48], it should be possible to use the AS-EphB TKI mice to identify direct kinase substrates of EphBs. Given the general limited knowledge of axon guidance mechanisms, identification of EphB substrates in the relevant neurons could be a powerful approach to uncover these mechanisms.

Our chemical genetic approach offers several advantages over conventional genetic loss-of-function studies[49]. Since we are able to block the kinase activity of EphBs while leaving their scaffolding and reverse signaling capabilities intact, it has been possible to dissect the role of the kinase activity of EphBs in vivo under conditions where EphBs are expressed at

physiological levels. As there are no Cre/lox-based conditional EphB mice of any kind yet available, the AS-EphB TKI mice represent an alternative for many experiments that require conditional regulation of EphB signaling. In addition, the reversible nature and the fine temporal control afforded by the chemical genetic approach should permit investigations into the functions of EphBs in the mature animal, such as in adult neurogenesis and synaptic plasticity, and in pathologies like Alzheimer's disease, autism and cancer[4,7,50]. This new window into EphB signaling should also provide insights crucial for therapeutic drug development for the treatment of EphB-mediated disease.

METHODS

Animals

EphB1^{T697G}, EphB2^{T699A}, and EphB3^{T706A} single mutants were generated individually by homologous recombination in mouse embryonic stem (ES) cells. Mice harboring each of the KI mutations were intercrossed to obtain the triple homozygous AS-EphB TKI mice.

To generate the targeting constructs, the 5' and 3' arms was PCR amplified from J1 ES cell DNA using primers listed in Supplementary Table 1 and subcloned into a modified pKSNeoDTA vector (originally constructed in the lab of Philippe Soriano) containing a loxP-Neo-loxP cassette for positive selection and a diptheria toxin A negative selection cassette (DTA). The AS mutations were introduced by site-directed mutagenesis. The targeting constructs were confirmed by sequencing. Linearized targeting construct was electroporated into J1 ES cells, which were subsequently selected with G418. Correct targeting of ES cells was initially screened by PCR and then confirmed by Southern analysis and direct sequencing of PCR products amplified from the mutated alleles. The positive clones were karyotyped and the Neo cassette was removed by electroporating targeted ES cells with a Cre expression plasmid. ES clones were microinjected into C57BL/6 blastocysts to generate chimeric mice. Male chimeric animals were mated to C57BL/6 wild-type females for germline transmission of the targeted allele.

The ES cell targeting efficiencies were as follows: EphB1 KI (17/192 = 9%), EphB2 KI (3/186 = 2%), EphB3 KI (12/96 = 13%).

Mice were maintained as homozygotes in a mixed 129/C57BL/6 background. Unless noted, wild-type (wild-type) mice were F1 offspring of a C57BL/6 x129sv cross. Animals were housed under a 12-hour light/dark cycle. No more than five animals were housed in each cage. Mice and embryos were chosen at random, regardless of sex, for treatment condition.

All experiments with mice were approved by the Animal Care and Use Committee of Harvard Medical School. Embryonic day 0 (E0) was defined as midnight preceding the morning a vaginal plug was found.

HEK 293 cell culture and transfection

HEK 293 cells were maintained in DMEM supplemented with 10% fetal bovine serum (Gibco), 2mM glutamine (Gibco), and penicillin/streptomycin (100 U/mL and 100 μg/mL, respectively; Gibco). HEK 293 cells were transfected using the calcium phosphate method as previously described[15].

Antibodies and Western blotting

The following antibodies were purchased commercially: pan-phospho-tyrosine pY99 mouse monoclonal (Santa Cruz); EphB1 (H-80) and EphB3 (H-85) rabbit polyclonal (Santa Cruz); β-actin mouse monoclonal (Abcam); PSD-95 mouse monoclonal (Pierce); synapsin rabbit

polyclonal (Millipore). Anti-neurofilament (2H3) mouse monoclonal antibody was obtained from the Developmental Studies Hybridoma Bank (from Thomas Jessell). Vav2, pan-phospho-EphB, and EphB2 rabbit polyclonal antibodies were generated in the Greenberg lab and described previously[15]. The phospho-specificity of the pan-phospho-EphB antibody was validated in HEK 293 cells for EphB1, EphB2, and EphB3 individually.

All Western blots were imaged and quantified using the Odyssey Infrared Imaging System (Licor) using fluorescently labeled secondary antibodies (Rockland Immunochemicals).

Protein binding assays

Full length human Grb2 and rat Pick1 were PCR amplified from Plasmids #26085 and #31613 (Addgene), respectively. Grb2 and Pick1 were fused to GST at their N-termini by cloning them into a pGEX vector (Pharmacia), expressed in E. coli, and affinity purified on glutathione sepharose beads. GST, used as the negative control, was expressed from the empty pGEX vector. EphB1AS protein was expressed in HEK 293 cells by transient transfection and treated with DMSO or 1 μM 1-NA-PP1 for 16 hrs. Cells were lysed in lysis buffer (30 mM Hepes pH 7.7, 100 mM KCl, 1 mM $MgCl_2$, 2 mM DTT, 2 mM sodium orthovandadate, 1% Triton X-100, protease inhibitor (Roche, 04693159001) and phosphatase inhibitor cocktails (Sigma, P5726, P0044)). The crude lysates were centrifuged at 40,000 rpm for 20 minutes at 4 degree C to generate the high-speed supernatants (HSS). HSS was incubated with glutathione beads coated with approximately GST, GST-Grb2 or GST-Pick1 with rotation at 4 degree C for 2 hours. The beads were washed 3 times with lysis buffer and analyzed by SDS-PAGE and Western blotting.

Pharmacology

1-NA-PP1 was synthesized as described previously[27] and dissolved in DMSO. 3-MB-PP1 was synthesized using a similar procedure and dissolved in DMSO. Dose response curves using 1-NA-PP1 and 3-MB-PP1 were calculated on GraphPad Prism using the least-squares method. The vehicle dose was calculated as two orders of magnitude below the lowest dose (=0.05 nM). For wild-type EphBs, 100% inhibition was defined at 1 mM.

Neuronal cell culture

Cortical and hippocampal neurons were prepared from E15-E17 mouse embryos as previously described[15]. Cultured neurons were maintained in Neurobasal Medium (Invitrogen) supplemented with 1× B27 (Invitrogen), penicillin/streptomycin (100 U/mL and 100 μg/mL, respectively) and 2mM glutamine. For biochemistry, neurons were seeded at a density of $2\times10^{\wedge6}$ neurons/well of a 6-well plate coated with polyornithine (Sigma). For electrophysiology and imaging, neurons were seeded at a density of $7.5\times10^{\wedge4}$ neurons/well on a glial monolayer on glass coverslips coated with polyornithine and laminin (Invitrogen).

Organotypic slices

Hippocampal organotypic slices were prepared in ice-cold dissection media (1 mM $CaCl_2$, 5 mM $MgCl_2$, 10mM D-glucose, 4 mM KCl, 26 mM $NaHCO_3$, 218 mM sucrose, 1.3 mM sodium phosphate, and 30 mM HEPES, pH 7.4). Brains were isolated from P5-7 pups, and hippocampi were excised and chopped into 400 μm sections. Slices were cultured on Millicell cell culture inserts (Millipore) in media containing 20% horse serum, 1 mM L-glutamine, 0.0012% ascorbic acid, 1 μg/mL insulin, 1 mM $CaCl_2$, 2 mM $MgCl_2$, 2.3 mg/mL glucose, 0.44 mg/mL $NaHCO_3$, 7.16 mg/mL HEPES in MEM.

Ephrin stimulation

For ephrin stimulations in dissociated cultured neurons and retinal explants, mouse ephrin-B1-Fc or ephrin-B2-Fc (R&D Systems) was pre-clustered for 50 minutes with goat anti-human IgG Fc (Jackson Immunoresearch) at room temperature in PBS at a molar ratio of 1:1 prior to stimulation. Pre-clustered ephrin-B1-Fc or ephrin-B2-Fc was added to the appropriate medium at a final concentration of 2.5 μg/mL. As a control, clustered human Fc in media was applied to neurons where specified.

Cell lysis and immunoprecipitation

Cultured cells were collected and homogenized in RIPA buffer (50 mM Tris pH 8.0, 150 mM NaCl, 1% Triton X-100, 0.5% Sodium Deoxycholate, 0.1% SDS, 10 mM NaF, complete protease inhibitor cocktail tablet (Roche), 1 mM sodium orthovanadate, and Phosphatase Inhibitor cocktails 1 and 2 (1×; Sigma). After clearing lysates, supernatants were incubated with the appropriate antibody for 1 hour at 4°C, followed by addition of Protein-A Fastflow agarose beads (Sigma) for 1 hour. Beads were washed in lysis buffer or PBS three times and eluted in 2× SDS sample buffer followed by boiling.

Surface labeling

Labeling of surface proteins was performed using the Pierce Cell Surface Protein Isolation Kit (Thermo Scientific). After chronic treatment with vehicle or 1 μM 1-NA-PP1, cultured cortical neurons were incubated with EZ-link biotin for 30 minutes at room temperature, washed with PBS, and lysed in RIPA buffer. Lysates were immunoprecipitated with an anti-EphB2 or control antibody, and probed with an anti-EphB2 antibody or fluorescently labeled streptavidin (Invitrogen).

Retinal explants

Ventrotemporal (VT) segments of retina were microdissected from E14.5 mouse embryos and cultured as previously described [51]. Embryos were removed from the uterus and decapitated, and heads were placed in ice-cold DMEM/F12 (Gibco). VT sections of the retina were excised and placed on glass coverslips coated with polyornithine and laminin. Explants were maintained in serum free medium (10 mg/mL BSA (Sigma), 1% ITS supplement (Sigma), Pen/Strep (20 U/mL and 20 μg/mL, respectively, Gibco) in DMEM/F12) supplemented with 0.2% methyl cellulose (Sigma) to increase media viscosity and minimize explant movement. All experiments were conducted 18–24 hour after initial plating.

Immunocytochemistry and growth cone collapse assay

For experiments with inhibitor treatment, explants were pre-incubated with vehicle or PP1 analogs for 1 hour, followed by a 30-minute ephrin-B2 stimulation, with variations as described in the text. Following stimulation, retinal explants were fixed for 20 minutes at 25°C with 4% paraformaldehyde (PFA)/2% sucrose in PBS. Explants were then blocked in 10% goat serum, 0.2% Tween-20 in PBS for 1 hour, followed by incubation with an anti-neurofilament antibody or anti-phospho-EphB antibody in 50% blocking solution overnight. After PBS washes, explants were incubated in Alexa Fluor-conjugated secondary antibodies (Invitrogen) and Alexa Fluor 488-conjugated phalloidin (Invitrogen). Explants on coverslips were mounted on glass slides using Fluoromount-G (Southern Biotech). Neurons were imaged using a laser scanning Zeiss Pascal microscope using a 40× objective with sequential acquisition settings at 1024 × 1024 pixel resolution. All imaging and image analysis were performed blind to the genotype and treatment condition of the samples. At least 10 growth cones were analyzed per explant.

In vivo 1-NA-PP1 delivery

Pregnant wild-type or AS-EphB TKI mice were injected subcutaneously twice daily with 80mg/kg 1-NA-PP1 dissolved in 10%DMSO, 20% Cremaphor-EL, 70% saline from E13.5 to E16.5 for optic tract experiments or from E12.5-E19 for cortical tract experiments. All experiments included data from at least two separate litters of embryos per condition. Animals used for in vivo 1-NA-PP1 treatment had no prior exposure to 1-NA-PP1 or other drugs.

DiI labeling

DiI labeling was performed as previously described[52]. At E16.5, embryo heads were fixed in 4%PFA /2% sucrose in PBS overnight and then washed with PBS. The lens and retina were removed from the left eye and a small crystal of DiI (Invitrogen) was placed in the optic disc. The retina was then replaced securely and the heads were stored in PBS+0.1% azide at room temperature for 12 days. After labeling, brains were removed and fluorescent optic tracts were imaged on a Leica MZ16F fluorescent stereomicroscope. Images were captured using Spot Advanced software. Labeling was quantified using Metamorph software by drawing rectangular regions of interest around the ipsilateral and contralateral tracts, subtracting background, and calculating the ipsilateral index based on integrated intensity of fluorescence:

ipsilateral index = ipsilateral / (ipsilateral + contralateral).

To compare wild-type and AS-EphB TKI responses with respect to 1-NA-PP1 treatment, each genotype was normalized to its untreated condition, producing a normalized ipsilateral index.

Analysis of corpus callosum phenotypes

E19.0 embryos were fixed in 4% PFA/2% sucrose in PBS for 2 days, then stored in PBS + 0.02% sodium azide at 4°C. Brains were removed and vibratome sectioned to 70 μm. Sections were blocked in 5% normal donkey serum, 1% BSA, 0.2% glycine, 0.2% lysine with 0.3% TritonX-100 in PBS at room temperature for 1 hour. To stain axon tracts, sections were incubated with rat anti-L1-CAM (Millipore, MAB5272MI) at a 1:200 dilution in blocking solution at 4°C overnight. Sections were washed three times with PBS and incubated with Cy3-conjugated donkey anti-rat IgG (Jackson) for 1.5 hours. Sections were washed 7–8 times with PBS and mounted with Aqua-mount (Lerner laboratories). Sections were imaged on an Olympus Bx51 epifluorescent microscope at 4× magnification. Corpus callosum partial agenesis was scored as the apparent failure of corpus callosal axons to cross the midline in a specific region along the rostral-caudal brain axis, and was evident by a gap in the dorsal midline region.

Quantitative PCR

Total RNA was isolated from mouse 7 DIV cortical cultures using Trizol reagent (Invitrogen) according to the manufacturer's instructions. Isolated RNA was treated with DNAseI Amplification Grade (Invitrogen) and a cDNA library was synthesized by cDNA High Capacity cDNA Reverse Transcription Kit (Applied Biosystems). The cDNA was the source of input for quantitative PCR, using a Step One Plus Real-Time PCR Instrument and SYBR Green reagents (Applied Biosystems). The relative expression plot was generated using concentration values that were normalized to corresponding actin concentrations. The following qPCR primer pairs were used:

EphB1-F- ACTGCAGAGTTGGGATGGAC

EphB1-R- CATCATAGCCACTGACTTCTTCC

EphB2-F- TTCATGGAGAACGGATCTCTG

EphB2-R- GACTGTGAACTGCCCATCG

EphB3-F- CCCTGGACTCCTTTCTACGG

EphB3-R- GCAATGCCTCGTAACATGC

Analysis of dendritic spines

For dissociated neuron experiments, cortical neurons were cultured as described above and grown on a monolayer of astrocytes on glass coverslips. Neurons were treated with vehicle or PP1 analogs at 10 DIV and media was changed entirely every 3–4 days (using neuronally pre-conditioned media). Neurons were transfected with GFP at 10 DIV using Lipofectamine 2000 and fixed with 4%PFA/2%sucrose in PBS at 21 DIV. Cells on coverslips were stained for GFP and mounted on slides using Fluoromount-G.

Neurons were imaged on a Zeiss Pascal confocal microscope, using a 63× objective, and maximal z-projections were analyzed using Metamorph software. Multiple sections of dendrite totaling > 50 μM were counted for each neuron.

For experiments in slice, hippocampal slices were treated with vehicle or PP1 derivatives at 2 DIV and media/drug were fully replaced every 2–3 days. At 2–3 DIV, plasmids encoding GFP (or GFP + EphB shRNAs) was biolistically transfected using a Helios gene gun. DNA bullets were prepared from 1.6 μm gold microcarrier particles (Biorad). After 8–9 DIV, slices were fixed in 3.2% PFA/5% sucrose in PBS for 1 hour and stained with chicken anti-GFP (Aves Labs) and rabbit anti-NeuN (Millipore) antibodies to visualize the structure of hippocampal fields. Basal and apical dendrites were analyzed separately and sections of dendrite totaling > 50 μM were counted for each neuron.

Electrophysiology

For experiments in dissociated neurons, whole-cell voltage clamp recordings were obtained using an Axopatch 200B amplifier at 25°C. During recordings, neurons were perfused with artificial cerebrospinal fluid containing 127 mM NaCl, 25 mM $NaHCO_3$, 1.25 mM Na_2HPO_4, 2.5 mM KCl, 2 mM $CaCl_2$, 1 mM $MgCl_2$, 25 mM glucose, and saturated with 95% O_2, 5% CO_2. Vehicle or 1-NA-PP1 treatment was initiated at 3 DIV and continued throughout recordings. The internal solution used in all eletrophysiological experiments contained 120 mM cesium methane sulfonate, 10 mM HEPES, 4 mM $MgCl_2$, 4 mM Na_2ATP, 0.4 mM Na_2GTP, 10 mM sodium phosphocreatine and 1 mM EGTA. Osmolarity and pH were adjusted to 310 mOsm and 7.3 with Millipore water and CsOH, respectively.

mEPSCs were isolated by exposing neurons to 0.5 μM tetrodotoxin, 50 μM picrotoxin, and 10 μM cyclothiazide (all from Tocris Bioscience). Cells with series resistance larger than 25 MΩ during the recordings were discarded. Data were analyzed in IgorPro (Wavemetrics) using custom-written macros. For each trace, the event threshold was set at 1.5 times the root-mean-square current. Currents were counted as events if they crossed the event threshold, had a rapid rise time (1.5 pA ms^{-1}) and had an exponential decay (tau<50 ms for mEPSC).

As a control for inhibition of EphBs, concurrent plates of neurons were treated with inhibitor and at the time of recording were stimulated with ephrin-B1 for 30 minutes. Neurons were lysed in 1× SDS-sample buffer, run on western blot and probed with rabbit anti-phospho-Eph and mouse anti-β-actin (Abcam) antibodies.

For mEPSC experiments in organotypic hippocampal slices, whole-cell voltage clamp recordings were made from visually identified CA1 pyramidal neurons and the mEPSC amplitude and frequency measured. Slices were treated with vehicle or 1-NA-PP1 from 2 DIV until the time of recording.

To evaluate evoked synaptic transmission, the Schafer collaterals were depolarized with an extracellular stimulating electrode and the postsynaptic evoked EPSC (eEPSC) response measured from CA1 neurons[53]. In these experiments the ACSF contained 4 mM Sr2+ instead of $CaCl_2$ and 4 mM $MgCl_2$ so that the extracellular stimulation resulted in asynchronous presynaptic vesicle fusion. The stimulus strength was set so that the initial postsynaptic response was 50–100pA and the current amplitude and frequency of the asynchronous EPSCs occurring 400–900 ms post-stimulation was measured. Slices were treated with vehicle or 1-NA-PP1 from 2 DIV until the time of recording. Analysis of eEPSCs was performed using custom-written macros in IgorPro.

Statistical Analysis

All animal experiments contained pups from multiple litters. All imaging analyses were done blind to condition. No data points were excluded in any experiment. Unpaired t-tests and 2-way ANOVA (for comparing effect of drug on AS EphB TKI neurons vs. wild-type) analyses were conducted using GraphPad Prism software. All tests are two-sided (standard). All error bars represent SEM.

Supplementary Material

Refer to Web version on PubMed Central for supplementary material.

Acknowledgments

We thank M. Thompson, Y. Zhou, and H. Ye of the Children's Hospital Boston I.D.D.R.C.M.G.M. facility for embryonic stem cell work and blastocyst injection, T. Kuwajima and the lab of Carol Mason for advice on retinal explants and DiI labeling, M. Lopez for help selecting and generating PP1 analogs, Z. Wills and A. Mardinly for help with synapse analysis, S. Cohen for advice on electrophysiological recordings, P. Zhang for assistance with animal management and L. Hu for antibody work.

This research was funded by NIH Grants RO1-NS-045500 (M.E.G.) and RO1-EY-018207 (C.W.C.). H.-Y.H.H. was supported by the Marion Abbe Fellowship of the Damon Runyon Cancer Research Foundation and NIH training grants in neurodegeneration and cancer biology. M.J.S. was supported by an NSF Graduate Research Fellowship. M.A.R. was supported by a training grant from NIDA (T32 DA07290).

REFERENCES

1. Klein R. Eph/ephrin signaling in morphogenesis, neural development and plasticity. Curr Opin Cell Biol. 2004; 16:580–589. [PubMed: 15363810]
2. Lai KO, Ip NY. Synapse development and plasticity: roles of ephrin/Eph receptor signaling. Curr Opin Neurobiol. 2009; 19:275–283. [PubMed: 19497733]
3. Genander M, Frisen J. Ephrins and Eph receptors in stem cells and cancer. Curr Opin Cell Biol. 2010; 22:611–616. [PubMed: 20810264]
4. Sanders SJ, et al. De novo mutations revealed by whole-exome sequencing are strongly associated with autism. Nature. 2012; 485:237–241. [PubMed: 22495306]
5. Merlos-Suarez A, Batlle E. Eph-ephrin signalling in adult tissues and cancer. Curr Opin Cell Biol. 2008; 20:194–200. [PubMed: 18353626]
6. Pasquale EB. Eph receptors and ephrins in cancer: bidirectional signalling and beyond. Nat Rev Cancer. 2010; 10:165–180. [PubMed: 20179713]
7. Cisse M, et al. Reversing EphB2 depletion rescues cognitive functions in Alzheimer model. Nature. 2011; 469:47–52. [PubMed: 21113149]

8. Sheffler-Collins SI, Dalva MB. EphBs: an integral link between synaptic function and synaptopathies. Trends Neurosci. 2012; 35:293–304. [PubMed: 22516618]
9. Henkemeyer M, et al. Nuk controls pathfinding of commissural axons in the mammalian central nervous system. Cell. 1996; 86:35–46. [PubMed: 8689685]
10. Grunwald IC, et al. Kinase-independent requirement of EphB2 receptors in hippocampal synaptic plasticity. Neuron. 2001; 32:1027–1040. [PubMed: 11754835]
11. Henderson JT, et al. The receptor tyrosine kinase EphB2 regulates NMDA-dependent synaptic function. Neuron. 2001; 32:1041–1056. [PubMed: 11754836]
12. Kayser MS, Nolt MJ, Dalva MB. EphB receptors couple dendritic filopodia motility to synapse formation. Neuron. 2008; 59:56–69. [PubMed: 18614029]
13. Kayser MS, McClelland AC, Hughes EG, Dalva MB. Intracellular and trans-synaptic regulation of glutamatergic synaptogenesis by EphB receptors. J Neurosci. 2006; 26:12152–12164. [PubMed: 17122040]
14. Himanen JP, Saha N, Nikolov DB. Cell-cell signaling via Eph receptors and ephrins. Curr Opin Cell Biol. 2007; 19:534–542. [PubMed: 17928214]
15. Dalva MB, et al. EphB receptors interact with NMDA receptors and regulate excitatory synapse formation. Cell. 2000; 103:945–956. [PubMed: 11136979]
16. Nolt MJ, et al. EphB controls NMDA receptor function and synaptic targeting in a subunit-specific manner. J Neurosci. 2011; 31:5353–5364. [PubMed: 21471370]
17. Palmer A, et al. EphrinB phosphorylation and reverse signaling: regulation by Src kinases and PTP-BL phosphatase. Mol Cell. 2002; 9:725–737. [PubMed: 11983165]
18. Henkemeyer M, Itkis OS, Ngo M, Hickmott PW, Ethell IM. Multiple EphB receptor tyrosine kinases shape dendritic spines in the hippocampus. J Cell Biol. 2003; 163:1313–1326. [PubMed: 14691139]
19. Orioli D, Henkemeyer M, Lemke G, Klein R, Pawson T. Sek4 and Nuk receptors cooperate in guidance of commissural axons and in palate formation. Embo J. 1996; 15:6035–6049. [PubMed: 8947026]
20. O'Donnell M, Chance RK, Bashaw GJ. Axon growth and guidance: receptor regulation and signal transduction. Annu Rev Neurosci. 2009; 32:383–412. [PubMed: 19400716]
21. Cowan CA, et al. Ephrin-B2 reverse signaling is required for axon pathfinding and cardiac valve formation but not early vascular development. Dev Biol. 2004; 271:263–271. [PubMed: 15223333]
22. Mendes SW, Henkemeyer M, Liebl DJ. Multiple Eph receptors and B-class ephrins regulate midline crossing of corpus callosum fibers in the developing mouse forebrain. J Neurosci. 2006; 26:882–892. [PubMed: 16421308]
23. Petros TJ, Shrestha BR, Mason C. Specificity and sufficiency of EphB1 in driving the ipsilateral retinal projection. J Neurosci. 2009; 29:3463–3474. [PubMed: 19295152]
24. Chenaux G, Henkemeyer M. Forward signaling by EphB1/EphB2 interacting with ephrin-B ligands at the optic chiasm is required to form the ipsilateral projection. Eur J Neurosci. 2011; 34:1620–1633. [PubMed: 22103419]
25. Ethell IM, et al. EphB/syndecan-2 signaling in dendritic spine morphogenesis. Neuron. 2001; 31:1001–1013. [PubMed: 11580899]
26. Bishop AC, et al. A chemical switch for inhibitor-sensitive alleles of any protein kinase. Nature. 2000; 407:395–401. [PubMed: 11014197]
27. Blethrow J, Zhang C, Shokat KM, Weiss EL. Design and use of analog-sensitive protein kinases. Chapter 18. Curr Protoc Mol Biol. 2004 Unit 18 11.
28. Chen X, et al. A chemical-genetic approach to studying neurotrophin signaling. Neuron. 2005; 46:13–21. [PubMed: 15820690]
29. Bishop AC, et al. Design of allele-specific inhibitors to probe protein kinase signaling. Curr Biol. 1998; 8:257–266. [PubMed: 9501066]
30. Alaimo PJ, Shogren-Knaak MA, Shokat KM. Chemical genetic approaches for the elucidation of signaling pathways. Curr Opin Chem Biol. 2001; 5:360–367. [PubMed: 11470597]

31. Rozakis-Adcock M, Fernley R, Wade J, Pawson T, Bowtell D. The SH2 and SH3 domains of mammalian Grb2 couple the EGF receptor to the Ras activator mSos1. Nature. 1993; 363:83–85. [PubMed: 8479540]
32. Moeller ML, Shi Y, Reichardt LF, Ethell IM. EphB receptors regulate dendritic spine morphogenesis through the recruitment/phosphorylation of focal adhesion kinase and RhoA activation. J Biol Chem. 2006; 281:1587–1598. [PubMed: 16298995]
33. Torres R, et al. PDZ proteins bind, cluster, and synaptically colocalize with Eph receptors and their ephrin ligands. Neuron. 1998; 21:1453–1463. [PubMed: 9883737]
34. Chumley MJ, Catchpole T, Silvany RE, Kernie SG, Henkemeyer M. EphB receptors regulate stem/progenitor cell proliferation, migration, and polarity during hippocampal neurogenesis. J Neurosci. 2007; 27:13481–13490. [PubMed: 18057206]
35. Yucel S, Dravis C, Garcia N, Henkemeyer M, Baker LA. Hypospadias and anorectal malformations mediated by Eph/ephrin signaling. J Pediatr Urol. 2007; 3:354–363. [PubMed: 18431460]
36. Risley M, Garrod D, Henkemeyer M, McLean W. EphB2 and EphB3 forward signalling are required for palate development. Mech Dev. 2009; 126:230–239. [PubMed: 19032981]
37. Choi Y, et al. Discovery and structural analysis of Eph receptor tyrosine kinase inhibitors. Bioorg Med Chem Lett. 2009; 19:4467–4470. [PubMed: 19553108]
38. Qiu R, et al. Regulation of neural progenitor cell state by ephrin-B. J Cell Biol. 2008; 181:973–983. [PubMed: 18541704]
39. Cowan CW, et al. Vav family GEFs link activated Ephs to endocytosis and axon guidance. Neuron. 2005; 46:205–217. [PubMed: 15848800]
40. Williams SE, et al. Ephrin-B2 and EphB1 mediate retinal axon divergence at the optic chiasm. Neuron. 2003; 39:919–935. [PubMed: 12971893]
41. Luria V, Krawchuk D, Jessell TM, Laufer E, Kania A. Specification of motor axon trajectory by ephrin-B:EphB signaling: symmetrical control of axonal patterning in the developing limb. Neuron. 2008; 60:1039–1053. [PubMed: 19109910]
42. Williams SE, Mason CA, Herrera E. The optic chiasm as a midline choice point. Curr Opin Neurobiol. 2004; 14:51–60. [PubMed: 15018938]
43. Bush JO, Soriano P. Ephrin-B1 regulates axon guidance by reverse signaling through a PDZ-dependent mechanism. Genes Dev. 2009; 23:1586–1599. [PubMed: 19515977]
44. Takasu MA, Dalva MB, Zigmond RE, Greenberg ME. Modulation of NMDA receptor-dependent calcium influx and gene expression through EphB receptors. Science. 2002; 295:491–495. [PubMed: 11799243]
45. McClelland AC, Sheffler-Collins SI, Kayser MS, Dalva MB. Ephrin-B1 and ephrin-B2 mediate EphB-dependent presynaptic development via syntenin-1. Proc Natl Acad Sci U S A. 2009; 106:20487–20492. [PubMed: 19915143]
46. Holmberg J, Frisen J. Ephrins are not only unattractive. Trends Neurosci. 2002; 25:239–243. [PubMed: 11972959]
47. Moon MS, Gomez TM. Balanced Vav2 GEF activity regulates neurite outgrowth and branching in vitro and in vivo. Mol Cell Neurosci. 2010; 44:118–128. [PubMed: 20298788]
48. Banko MR, et al. Chemical Genetic Screen for AMPKalpha2 Substrates Uncovers a Network of Proteins Involved in Mitosis. Mol Cell. 2011; 44:878–892. [PubMed: 22137581]
49. Knight ZA, Shokat KM. Chemical genetics: where genetics and pharmacology meet. Cell. 2007; 128:425–430. [PubMed: 17289560]
50. Batlle E, et al. EphB receptor activity suppresses colorectal cancer progression. Nature. 2005; 435:1126–1130. [PubMed: 15973414]
51. Petros TJ, Bryson JB, Mason C. Ephrin-B2 elicits differential growth cone collapse and axon retraction in retinal ganglion cells from distinct retinal regions. Dev Neurobiol. 2010; 70:781–794. [PubMed: 20629048]
52. Plump AS, et al. Slit1 and Slit2 cooperate to prevent premature midline crossing of retinal axons in the mouse visual system. Neuron. 2002; 33:219–232. [PubMed: 11804570]

53. Xu-Friedman MA, Regehr WG. Presynaptic strontium dynamics and synaptic transmission. Biophys J. 1999; 76:2029–2042. [PubMed: 10096899]

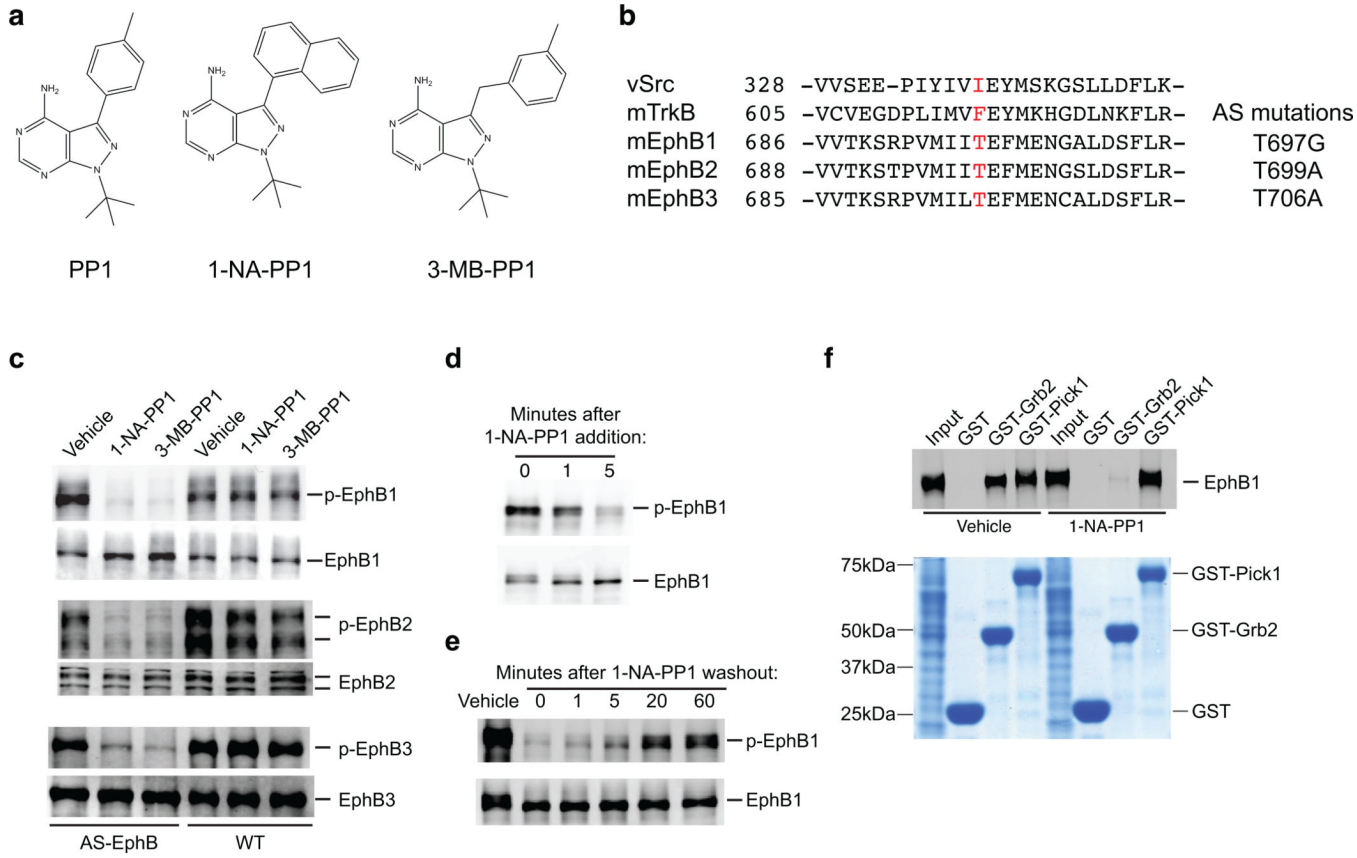

Figure 1. A chemical genetic approach to studying EphB signaling

(a) Chemical structures of the Src inhibitor PP1 and its analogs 1-NA-PP1 and 3-MB-PP1.

(b) Amino acid alignment of kinase domains of mouse EphBs with those of avian vSrc and mouse TrkB. The gatekeeper residue is highlighted in red and the PP1 analog-sensitive (AS) mutation made in the EphBs is shown on the right.

(c) Inhibition of the kinase function of AS-EphB proteins. HEK 293 cells expressing the AS or wild-type versions of EphB1, EphB2 and EphB3 were incubated with 1-NA-PP1 (250 nM) or 3-MB-PP1 (1 μM) for 1 hour. Cell lysates were analyzed by Western blotting for total EphBs or tyrosine phosphorylated EphBs.

(d) Time course of AS-EphB1 inhibition after 1-NA-PP1 (250 nM) addition to AS-EphB1-expressing HEK 293 cells.

(e) Time course of recovery of AS-EphB1 auto-phosphorylation after 1-NA-PP1 (250 nM) washout from AS-EphB1-expressing HEK 293 cells. The zero time point reflects the moment of 1-NA-PP1 washout after an initial 1-hour incubation.

(f) Effect of 1-NA-PP1 on the ability of AS-EphB1 to bind Grb2 or Pick1. HEK 293 cells expressing AS-EphB1 were incubated with either vehicle or 1-NA-PP1. Cell lysates were incubated with GST, GST-Grb2 or GST-Pick1 proteins immobilized on glutathione beads. Proteins bound to the beads were analyzed by Western blotting for EphB1 (top of gel). The same gel (bottom) was stained with Coomassie blue to verify that similar amounts of GST fusion proteins were present in the binding reactions. Uncropped blots are shown in Supplementary Figure 7.

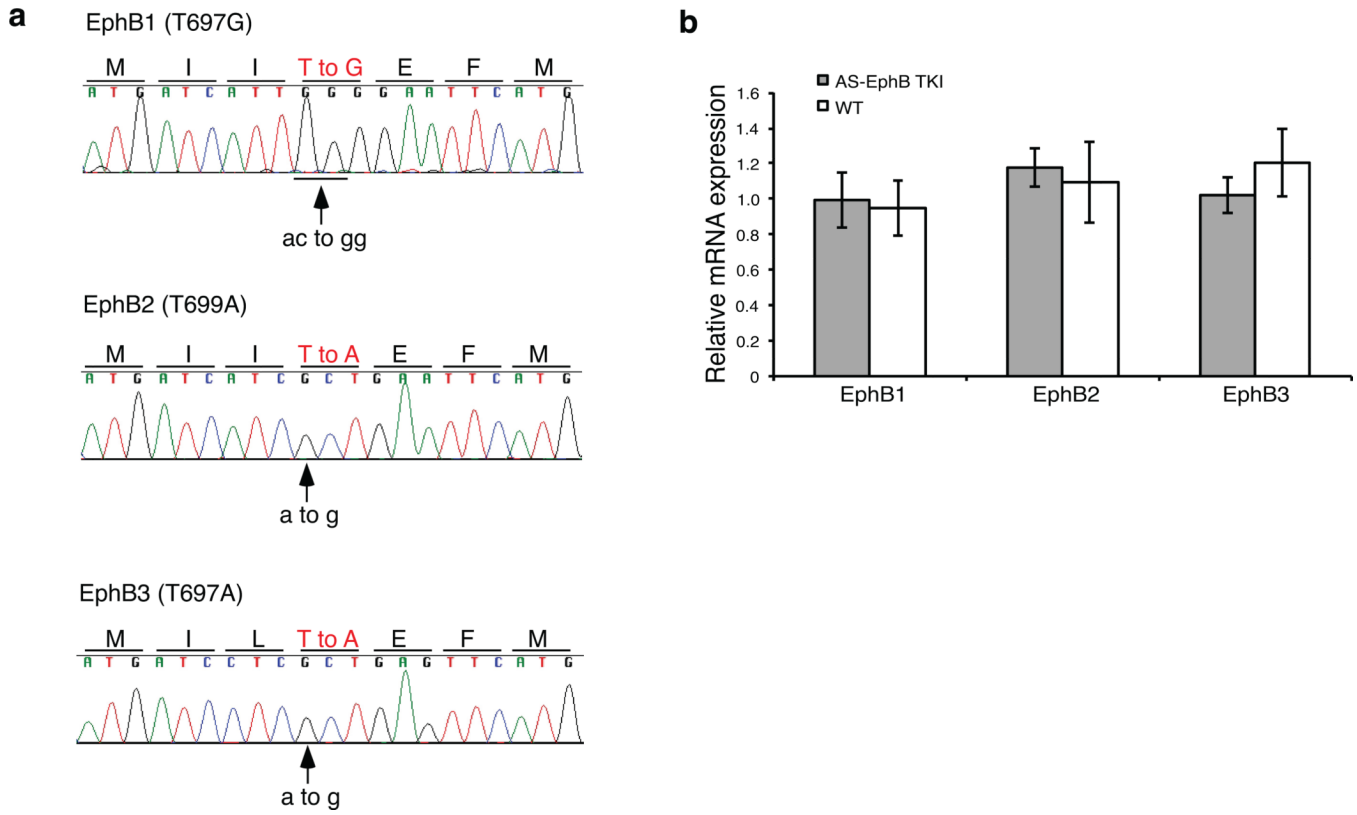

Figure 2. Generation of AS-EphB TKI mice

(a) Sequencing reads from AS-EphB knockin mouse embryonic stem cells showing the gatekeeper (AS) mutation in the *Ephb1, Ephb2*, and *Ephb3* genes. The mutated amino acids are shown in red. The arrows indicate the DNA base substitutions.

(b) Relative mRNA expression of EphB1, EphB2, and EphB3 normalized to β-actin in AS-EphB TKI vs. wild-type cultured cortical neurons. Data are mean of two biological replicates ± SEM.

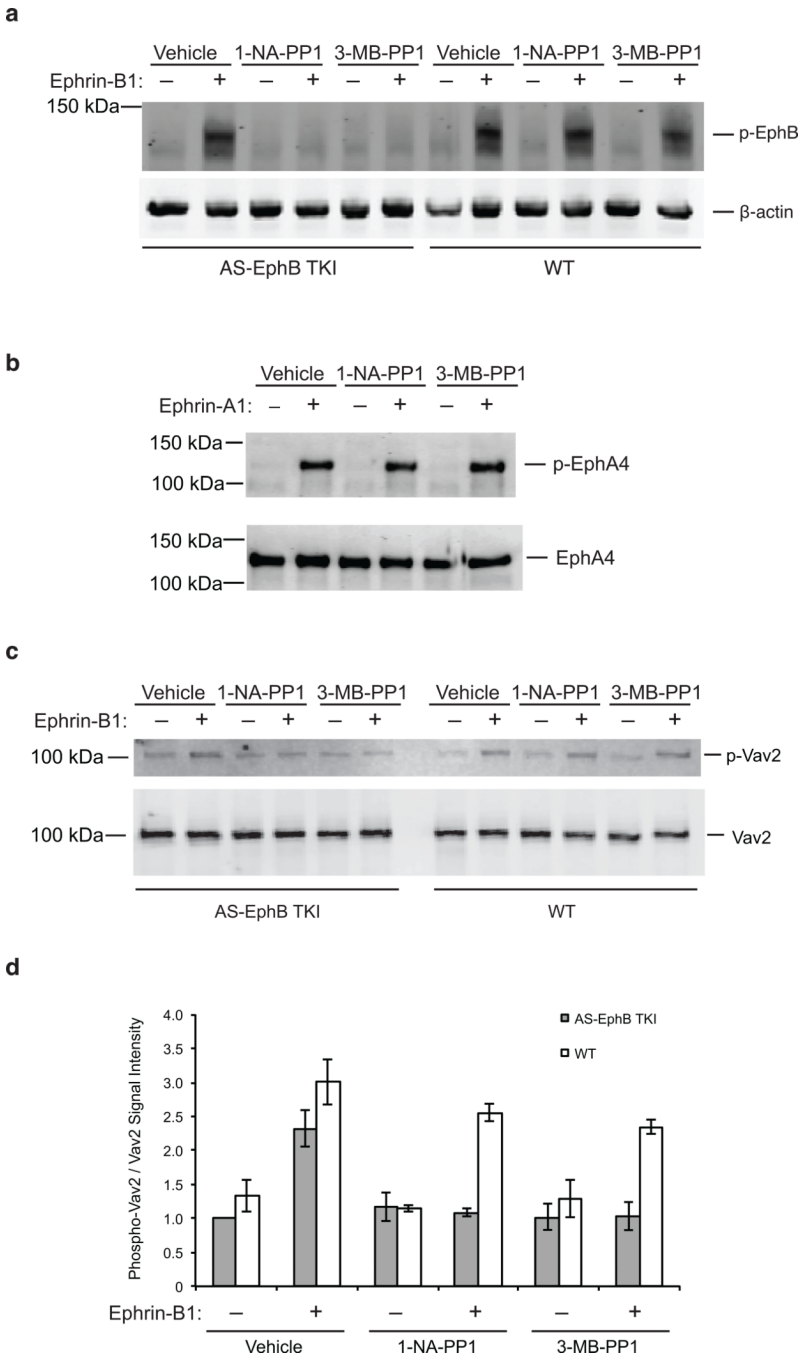

Figure 3. Selective inhibition of the kinase function of EphBs in AS-EphB TKI mice

(a) Inhibition of the EphB kinase activity in AS-EphB TKI neurons. 15 day in vitro (DIV) dissociated AS-EphB TKI embryonic cortical neurons were pre-incubated with vehicle, 250 nM 1-NA-PP1, or 1 μM 3-MB-PP1 for 1 hour before a 30-minute ephrin-B1 stimulation. Cell lysates were then analyzed by Western blotting for phospho-EphB or β-actin.

(b) Effect of PP1 analogs on the kinase activity of EphA4. 4 DIV cortical neurons were pre-incubated with vehicle, 250 nM 1-NA-PP1, or 1 μM 3-MB-PP1 for 1 hour before a 30-minute ephrin-A1 stimulation. Lysates were immunoprecipitated with an anti-EphA4 antibody and blotted for phospho-EphA4 and EphA4.

(c) Effect of PP1 analogs on ephrin-B1-induced Vav2 phosphorylation. 4 DIV AS-Eph TKI or wild-type cortical neurons were stimulated with ephrin-B1, immunoprecipitated with an anti-Vav2 antibody, and blotted with a pan-phospho-tyrosine (pY99) or Vav2 antibody. Cells were pre-incubated with vehicle, 250 nM 1-NA-PP1, or 1 μM 3-MB-PP1 for 1 hour before a 30-min ephrin-B1 stimulation.
(d) Quantification of phospho-Vav2/Vav2 band intensity from quantitative western blots in (c). Data are mean ± SEM (n=3 biological replicates). Values were normalized to the unstimulated AS-EphB TKI vehicle-treated condition.
Uncropped blots are shown in Supplementary Figure 7.

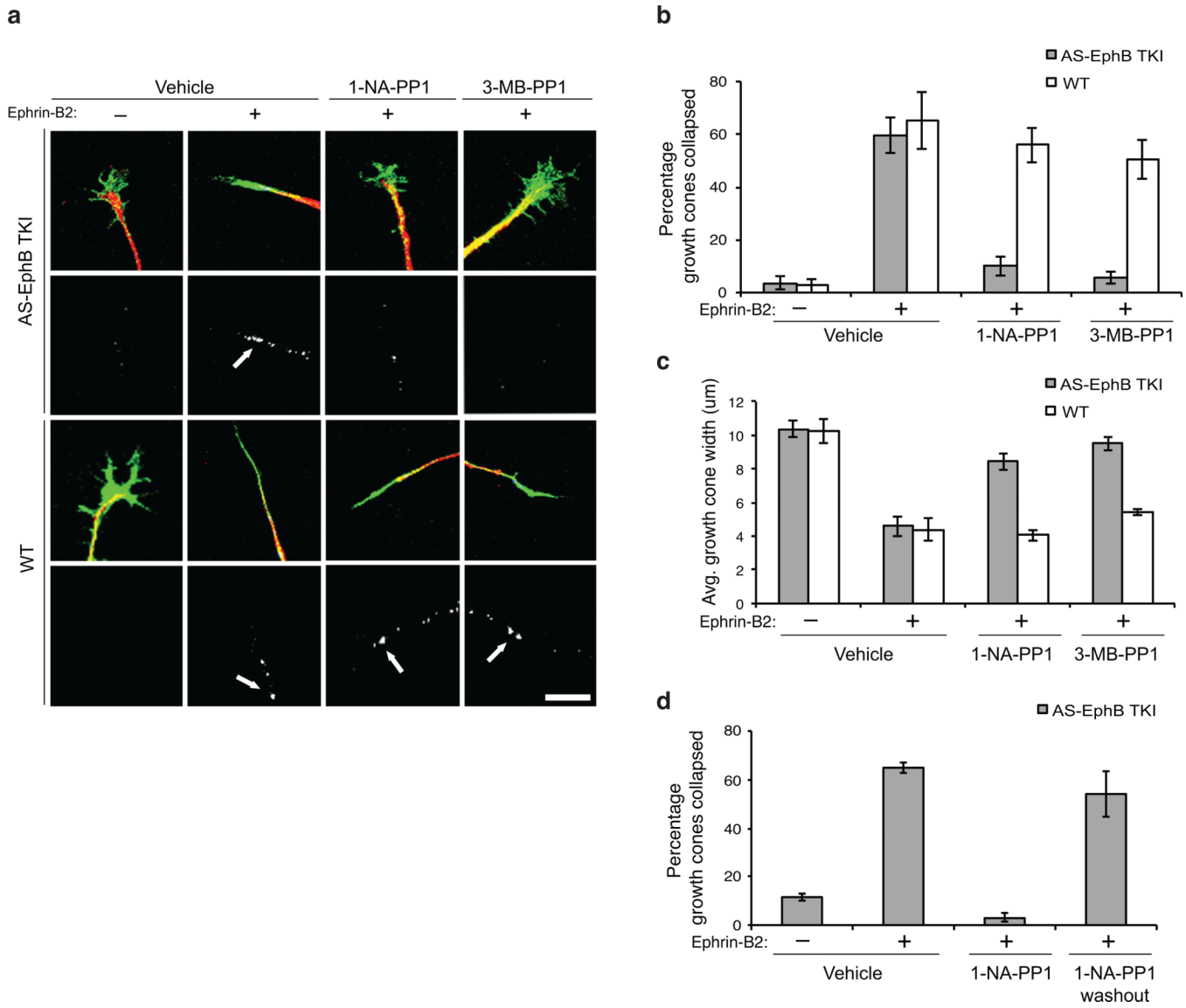

Figure 4. The kinase function of EphBs is required for growth cone collapse in ventrotemporal (VT) retinal ganglion cells

All data are mean ± SEM. N=4–8 explants (biological replicates) per condition for each experiment.

(a) Effect of PP1 analog on RGC growth cone collapse. Embryonic day 14 (E14) VT retinal explants were treated with vehicle, 250 nM 1-NA-PP1, or 1 μM 3-MB-PP1 before ephrin-B2 stimulation. Explants were stained for neurofilament (red), phospho-EphB (white) and labeled with phalloidin to visualize F-actin (green). White arrows denote clusters of phospho-EphB staining. Scale bar represents 10 μm.

(b) Quantification of the percentage of collapsed growth cones from (a). A 2-way ANOVA revealed a significant interaction between genotype and inhibitor treatment in each condition, indicating that the effects of inhibitors were significantly greater in AS-EphB TKI neurons than in wild-type neurons: vehicle vs. 1-NA-PP1: $F_{(1,20)}$=6.66, p=.018; vehicle vs. 3-MB-PP1: $F_{(1,22)}$=7.41, p=.012.

(c) Quantification of the average growth cone width from (a). A 2-way ANOVA revealed a significant interaction between genotype and inhibitor treatment in each of the conditions:

vehicle vs. 1-NA-PP1: $F_{(1,20)}$=11.75, p=.0027; vehicle vs. 3-MB-PP1: $F_{(1,22)}$=11.49, p=.0026.

(d) Quantification of the percentage of collapsed growth cones after 1-NA-PP1 washout. Retinal explants were treated with 250 nM1-NA-PP1 as in (a), but 15 minutes into a 30-minute ephrin-B2 stimulation, media were removed and replaced with fresh media containing vehicle. Percentage of collapsed growth cones was then quantified as in (b).

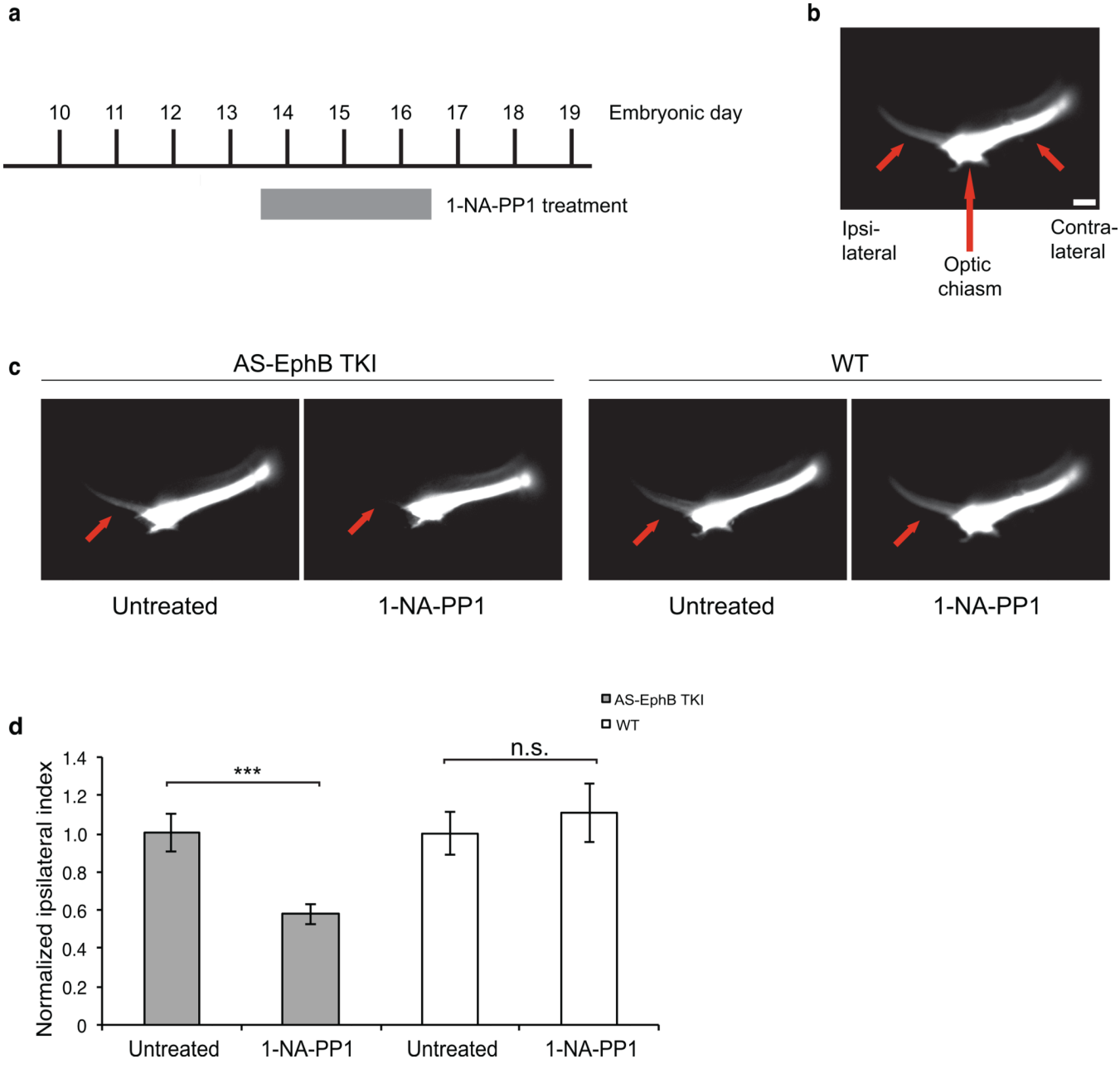

Figure 5. The kinase function of EphBs is required for the formation of the ipsilateral retinal projection in vivo

(a) Schedule of in vivo 1-NA-PP1 administration. Twice-daily subcutaneous injections of 80 mg/kg 1-NA-PP1 were administered to pregnant females from E13.5–16.5.

(b) Representative image demonstrating the orientation of the ipsilateral and contralateral retinal projections (short red arrows) of the optic tract with respect to the optic chiasm (long red arrow) as visualized by DiI labeling (white). Scale bar represents 100 μm.

(c) Representative images of DiI-filled retinal projections at E16.5. Pregnant AS-EphB and C57BL/6 wild-type mice were treated as described in (a). Red arrows denote the ipsilateral projection.

(d) Quantification of the ipsilateral phenotype shown in (c). The Ipsilateral Index is defined as: ipsilateral / (ipsilateral + contralateral) fluorescence intensity and normalized for each

genotype. The number of embryos examined was as follows: Untreated AS-EphB TKI (n=30), 1-NA-PP1 treated AS-EphB TKI (n=30), Untreated wild-type (n=15), 1-NA-PP1-treated wild-type (n=17). ***, p<.001; n.s., not significant by Student's t-test. A 2-way ANOVA revealed a significant interaction between genotype and inhibitor treatment, indicating that 1-NA-PP1 treatment effects were significantly greater in AS-EphB TKI embryos than in wild-type embryos ($F_{(1,88)}$=6.5, p=.0125). Data are mean ± SEM. Samples are biological replicates.

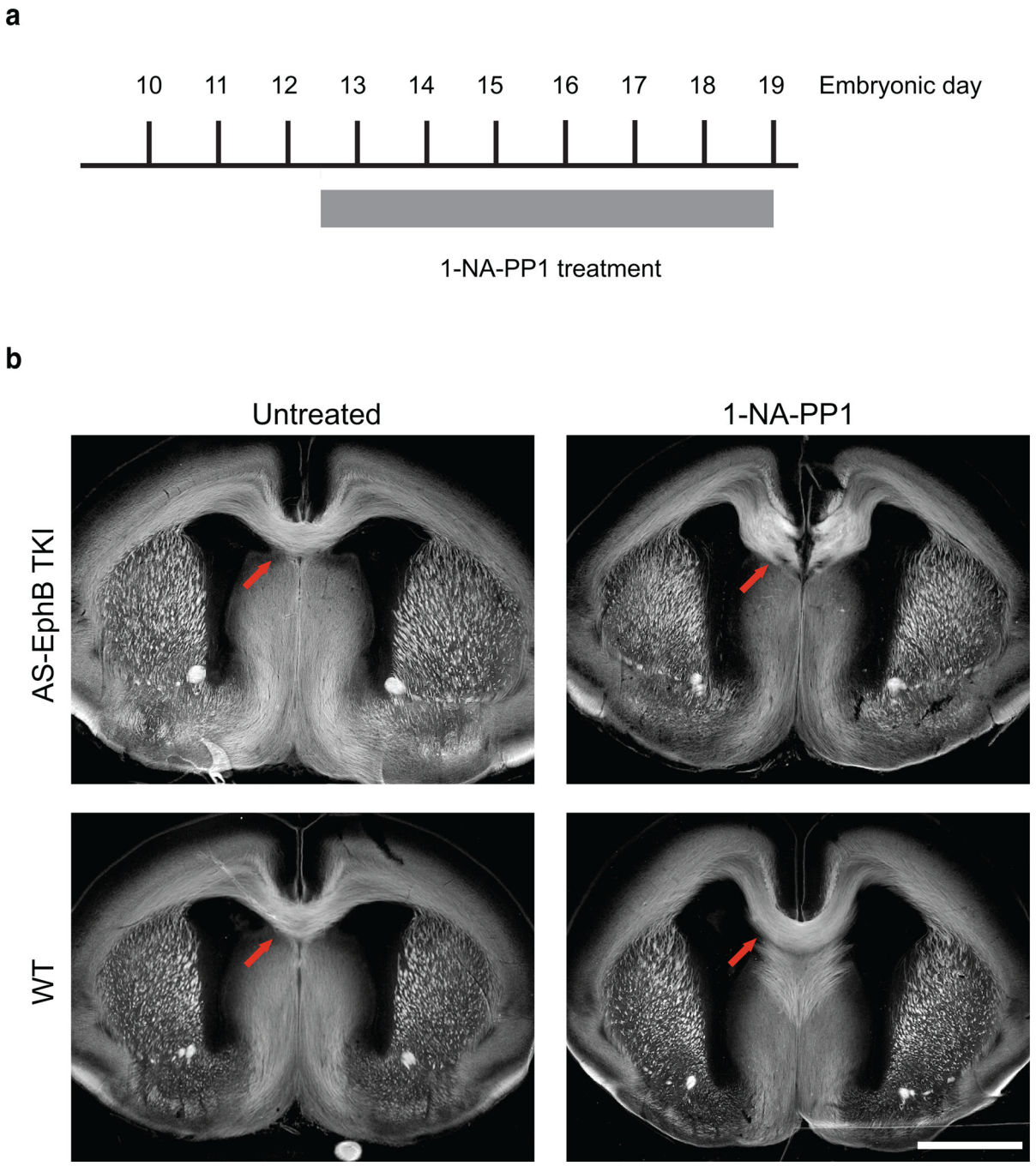

Figure 6. The kinase activity of EphBs is required for the formation of the corpus callosum in vivo

(a) Schedule of in vivo 1-NA-PP1 administration. Twice-daily subcutaneous injections of 80 mg/kg 1-NA-PP1 were administered to pregnant mice from E12.5–E19.

(b) Representative images of brain sections from E19 embryos stained with L1-CAM antibody (white) to visualize axon tracts. Red arrows denote the corpus callosum. Scale bar represents 1 mm.

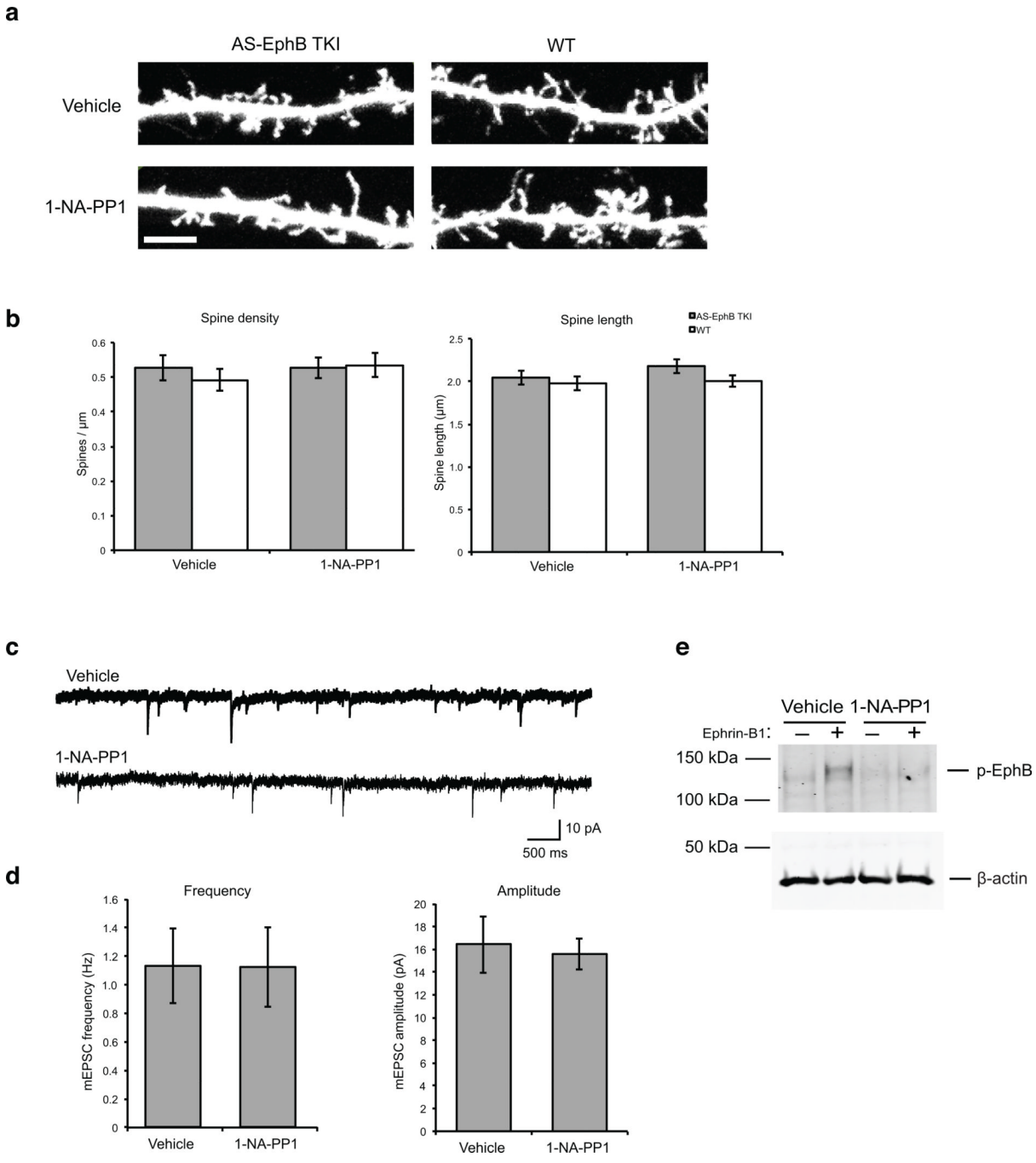

Figure 7. The kinase activity of EphBs is dispensable for the formation of dendritic spines and functional excitatory synapses in culture

(a) Representative images of dendritic spines from cultured AS-EphB TKI and wild-type cortical neurons treated with vehicle or 1 μM 1-NA-PP1 from 10–21 DIV. Neurons were transfected at 10 DIV with GFP and stained with an anti-GFP antibody. Scale bar represents 5 μm

(b) Quantification of spine density and spine length from (a). Data are mean ± SEM. N = 25–33 neurons from independent biological replicates/condition.

(c) Representative traces of recordings of miniature postsynaptic excitatory currents (mEPSCs) from dissociated cortical neurons from AS-EphB TKI embryos at 10–12 DIV.

Cultures were treated with vehicle or 1-NA-PP1 (1 μM) from 3 DIV until the time of recording.

(d) Quantification of mEPSC frequency and amplitude from vehicle and 1-NA-PP1 treated neurons. Data are mean ± SEM. N=13 cells from independent biological replicates/ condition.

(e) The tyrosine kinase activity of AS-EphBs is inhibited by 1-NA-PP1. Cultures concurrent with those used in (d) were treated with 1-NA-PP1 under identical culture conditions then stimulated for 30 minutes with ephrin-B1 at 10 DIV. Cell lysates were analyzed by western blotting for phospho-EphB and β-actin. Uncropped blots are shown in Supplementary Figure 7.

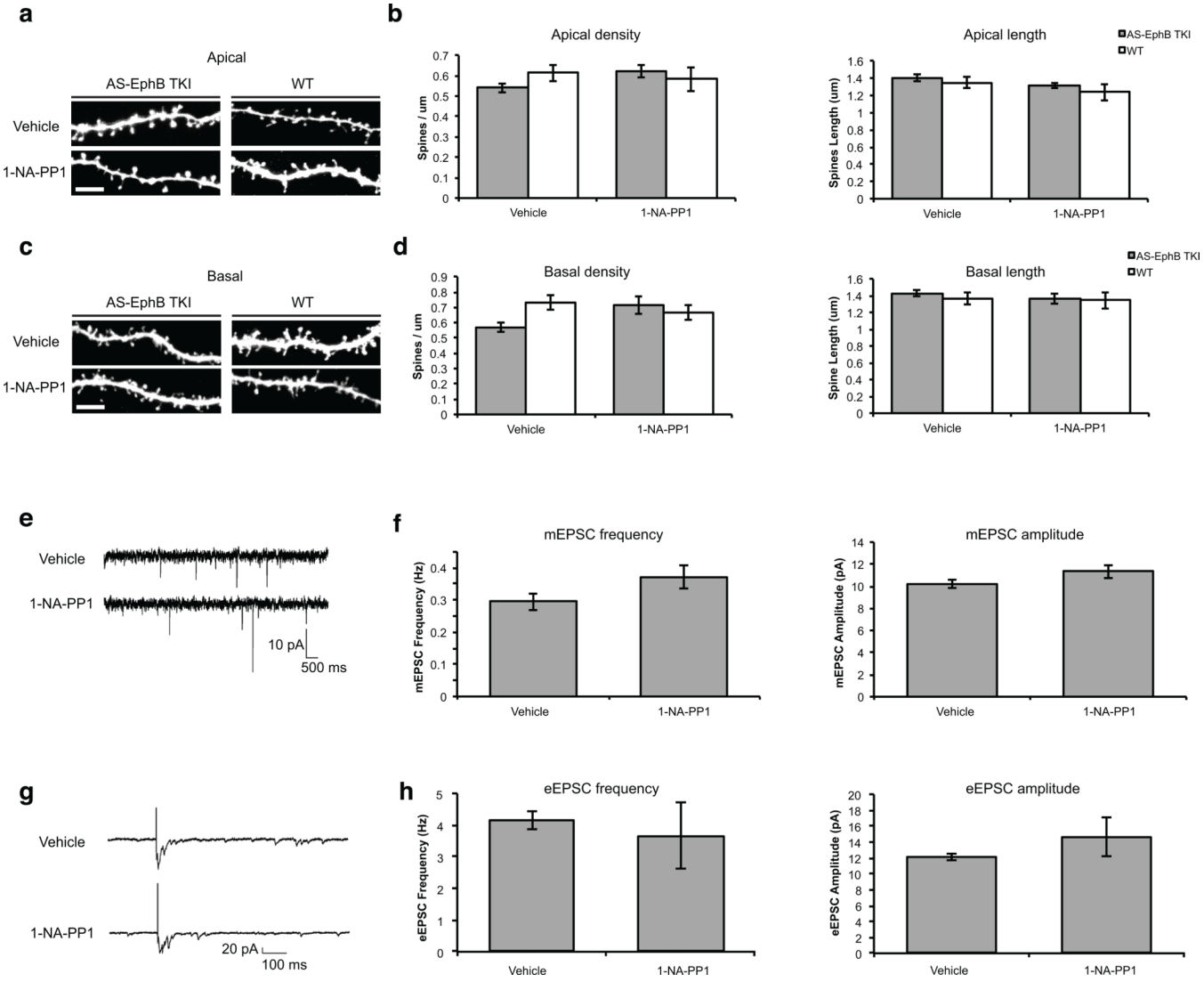

Figure 8. The kinase activity of EphBs is dispensable for the formation of dendritic spines and functional excitatory synapses

All experiments were done in organotypic hippocampal slices. The concentration of 1-NA-PP1 is 1μM. All data are mean ± SEM. Samples are independent biological replicates.

(a) Representative images of apical spines from AS-EphB TKI slices. Slices from P5–7 mice were treated with vehicle or 1-NA-PP1 from 0–8 DIV. Scale bar represents 5 μm

(b) Quantification of apical spine density and spine length from (a). N (neurons) = wild-type Vehicle (21), wild-type 1-NA-PP1 (11), AS-EphB TKI Vehicle (30), AS-EphB TKI1-NA-PP1 (16).

(c) Representative images of basal spines from slices as described in (a).

(d) Quantification of basal spine density and spine length from (c).

(e) Representative traces from recordings of mEPSCs from P5–7 AS-EphB TKI slices at 12–14 DIV.

(f) Quantification of mEPSC frequency and amplitude from (e). N (neurons) = AS-EphB TKI Vehicle (16), AS-EphB TKI 1-NA-PP1 (19).1-NA-PP1 did not produce a significant change in mEPSC frequency or amplitude by Student's t-test.

(g) Representative traces from recordings of eEPSCs from P5–7 AS-EphB TKI slices at 12–14 DIV.

(h) Quantification of eEPSC frequency and amplitude in hippocampal slices. N (neurons) = AS-EphB TKI Vehicle (7), AS-EphB TKI 1-NA-PP1 (7). 1-NA-PP1 did not produce a significant change in eEPSC frequency or amplitude by Student's t-test.